Gain-of-function Shh mutants activate Smo *in cis* independent of Ptch1/2 function

Catalina Casillas and Henk Roelink

Department of Molecular and Cell Biology, 16 Barker Hall, 3204, University of California, Berkeley CA 94720, USA

roelink@berkeley.edu

Abstract

Sonic Hedgehog (Shh) signaling is characterized by strict non-cell autonomy; cells expressing Shh do not respond to their ligand. Here, we identify several Shh mutations that gain the ability to activate the Hedgehog (Hh) pathway *in cis*. This activation requires the extracellular cysteine rich domain of Smoothened, but is otherwise independent of Ptch1/2. Many of the identified mutations disrupt either a highly conserved catalytic motif found in peptidases or an α-helix domain frequently mutated in holoprosencephaly-causing *SHH* alleles. The expression of gain-of-function mutants often results in the accumulation of unprocessed Shh pro-peptide, a form of Shh we demonstrate is sufficient to activate the Hh response cell-autonomously. Our results demonstrate that Shh is capable of activating the Hh pathway via Smo independently of Ptch1/2, and that it harbors an intrinsic mechanism that prevents cell-autonomous activation of the pathway to favor non-cell autonomous signaling.

Introduction

Sonic Hedgehog (Shh) is a signaling molecule indispensable for vertebrate embryonic development and adult stem cell maintenance. Impaired regulation of the Hedgehog (Hh) pathway can cause of various birth defects and diseases, including Holoprosencephaly (HPE) and a several of tumor types (Bale, 2002). Shh is synthesized as a 45 kDa pro-peptide encompassing a signaling "Hedge" domain and an intein-like "Hog" domain at the C-terminal end. Previous work has shown that the "Hog" domain mediates an autocatalytic cleavage of Shh, resolved only by the addition of a cholesterol moiety on the C-terminus of the 19 kDa "Hedge" domain ($ShhN_{Chol}$) (Lee et al., 1994). $ShhN_{Chol}$ becomes further modified with the attachment of a palmitoyl group to its N-terminus (Buglino and Resh, 2008). Lipid modified $ShhN_{Chol}$ is then secreted from expressing cells through a mechanism requiring Dispatched1 (Disp1), Scube2, and ADAM metalloproteases. The release of $ShhN_{Chol}$ from cell membranes requires the removal of its lipid modifications, which results in soluble and biologically active ligands capable of non-cell autonomous signaling (Jakobs et al., 2014; Ohlig et al., 2012).

In the absence of Shh ligand, the receptors Patched1 (Ptch1) and Patched2 (Ptch2) inhibit the signal transducer Smoothened (Smo) through a sub-stoichiometric mechanism (Alfaro et al., 2014a; Taipale et al., 2002; J. Zhang et al., 2001). Ptch1 and Ptch2, as well as Boc, Cdo, and Gas1, are required extracellular Shh receptors that regulate the Hh responses *in vivo* (Allen et al., 2011; Goodrich et al., 1997; Izzi et al., 2011). The binding interface between Shh and Ptch1, as well as the Shh antagonist Hhip (Bosanac et al., 2009), encompasses a Zn^{2+} ion coordinated within Shh that is part of a larger and highly conserved motif resembling a zinc peptidase catalytic domain (Hall et al., 1995a). The conserved catalytic site, and consequently any putative enzymatic activity, has been shown not to be required for non-cell autonomous, or *in trans*, signaling (Fuse et al., 1999); thus it is often referred to as a "pseudo active" site in Shh. The binding interface between Shh and its co-receptors, Boc, Cdo, and Gas-1, incorporates a portion of the catalytic domain that chelates two Ca^{2+} ions (McLellan et al., 2008). Accordingly, mutations that disrupt Ca^{2+} chelation (such as E90A (Izzi et al., 2011)) interfere with the binding of Shh to Boc, Cdo, and Gas1, and have been used to demonstrate the requirement for co-receptor binding to initiate the Hh response *in trans*.

The binding of Shh to a receptor complex on the surface of receptive cells leads to its internalization and the disinhibition of Smo, an event that results in changes to the subcellular distribution and activity of the signal transducer. The mechanism that links the extracellular binding of Shh to the activation of predominantly intracellular Smo is enigmatic (Aanstad et al., 2009; Bijlsma et al., 2012;

Incardona et al., 2002; 2000; Milenkovic et al., 2009). Smo is a Class F G-protein coupled receptor (GPCR) and belongs to a receptor superfamily predominantly defined by Frizzleds (Frz), the canonical receptors of the Wnt pathway (Bhanot et al., 1996; Kristiansen, 2004). Smo and Frzs share over 25% sequence identity; both contain a characteristic heptahelical domain as well as a conserved extracellular Cysteine Rich Domain (CRD). Wnts bind to the CRD of Frz receptors through two distinct binding sites, one of which is a protein-lipid interface, to initiates signal transduction (Janda et al., 2012). Although Ptch1-mediated inhibition of Smo is thought to target a specific hydrophobic binding pocket within the heptahelical domain of Smo, the CRD of Smo can also regulate Hh pathway activity by binding to a variety of sterols- most of which cause an activation of the response (Myers et al., 2013; Nachtergaele et al., 2013; Nedelcu et al., 2013) (Corcoran and Scott, 2006; Huang et al., 2016; Xiao et al., 2017). The regulatory interactions involving the CRD of Smo demonstrate that activation of the Hh pathway is multifaceted, and that Ptch1-mediated inhibition is only part of a more complex regulation of Smo activity.

In this study, we find that expression of several Shh mutants activates the transcriptional Hh response cell-autonomously in *Ptch1*$^{LacZ/LacZ}$;*Ptch2*$^{-/-}$ cells. *Ptch1*$^{LacZ/LacZ}$;*Ptch2*$^{-/-}$ cells also retain the ability to migrate towards a source of ShhN, a non-canonical Hh response mediated by Smo. We demonstrate that this Shh-mediated activation events occur independently of all canonical Shh receptors, but requires the CRD of Smo. Many of the Shh mutants that activate the Hh response exhibit defects in processing resulting in the perdurance of Shh pro-protein. This Shh pro-protein retains its activity when expressed in the developing neural tube. Our results demonstrate that many Shh mutants are capable of activating the Hh response via Smo independent of Ptch1/2 function. As the amount of Shh pre-protein, but $ShhN_{Chol}$, correlates with the level of cell-autonomous Smo activation, it appears that auto-processing of Shh turns the active Shh pre-protein into the inactive $ShhN_{Chol}$. This form of Shh can be re-activated by the removal of the cholesterol moiety.

Results

Shh can activate the Hh response cell-autonomously independent of the canonical receptors

Signaling by Shh is strictly non-cell autonomous (García-Zaragoza et al., 2012; Shaw et al., 2009; Yauch et al., 2008). In SHH-induced tumors, the non-SHH-expressing cells are sensitive to Smo inhibitors, whereas cells expressing Shh are not. This notion of non-autonomy in Shh signaling is further supported by the observation that in embryos, cells that express Shh (e.g. cells in the notochord and floor plate) do not express *Ptch1*, a gene that is universally upregulated in cells responding to Shh. As *Ptch1* is not expressed in cells expressing Shh, we set out to test if the absence of this receptor causes the inability of cells to respond to Shh. To assure lack of all Ptch

activity, we used *Ptch1*$^{LacZ/LacZ}$;*Ptch2*$^{-/-}$ cells. These Ptch1/2-deficient cells do not induce the transcriptional Hh response when exposed to exogenously supplied ShhN (Roberts et al., 2016), which also ensures that any Hh pathway activity we measure is strictly cell-autonomous.

To similarly assess the requirement of Shh (co-)receptors to activate the Hh response, we used Shh-E90A (a mutant unable to bind to Boc, Cdo, and Gas1(Allen et al., 2011; Izzi et al., 2011)) and Shh-H183A a mutant that breaks the Zn^{2+} triad, which interferes with Hhip and Ptch1 binding. Both *Shh* and its mutant forms effectively induced the transcriptional Hh response after transfection in *Ptch1*$^{LacZ/LacZ}$;*Ptch2*$^{-/-}$ cells (Figure 1A). To unambiguously demonstrate that the Shh co-receptors are not required for *in cis* activation of the Hh response, we used *Ptch1*$^{LacZ/LacZ}$;*Ptch2*$^{-/-}$;*Boc*$^{-/-}$;*Cdo*$^{-/-}$;*Gas1*$^{-/-}$;*Shh*$^{-/-}$ cells. Upon neuralization ES cells with this genotype have an activated Shh response (Figure 1C), consistent with their lack of Ptch1/2. We transfected fibroblasts derived from the *Ptch1*$^{LacZ/LacZ}$;*Ptch2*$^{-/-}$;*Boc*$^{-/-}$;*Cdo*$^{-/-}$;*Gas1*$^{-/-}$;*Shh*$^{-/-}$ ES cells with *Shh, ShhN* and their *-E90A* and *-H183A* mutant derivatives. We found that also in these receptorless cells the Hh response could be induced by these froms of Shh (Figure 1D). The ability of Shh and ShhN to induce the Hh response was shared with Ihh and Dhh (Figure 1E). These results demonstrate that activation of the Hh response *in cis* can occur independent of canonical (co-)receptors.

Shh protein was readily detected in transfected *Ptch1*$^{LacZ/LacZ}$;*Ptch2*$^{-/-}$ cells (Figure 1B). In these cells, Shh is normally processed into a cholesterol-associated form ($ShhN_{Chol}$) (19 kD), but full-length Shh pro-protein (45 kD) can be detected as well. Cells expressing Shh-H183A had little N-terminal processed Shh, and comparable levels of full length pro-protein (Figure 1B). It thus appears that the ability to induce the transcriptional Hh response *in cis* correlates with the presence of the full length form of Shh, and not with the N-terminal processed form. To determine if unprocessed Shh pro-protein could mediate the activation of the Hh response *in cis*, we tested Shh-C199S, a form of Shh largely unable to undergo autoproteolysis (Figure 1B) and found that this mutant was an equally potent inducer of the Hh response (Figure 1A). As cholesterol-modified ShhN ($ShhN_{Chol}$) is only activated upon shedding and removal of its lipid moieties (Ohlig et al., 2011), we tested a form of Shh that does not have the cholesterol moiety (Shh-C199* or ShhN), and does not require an activation event. We found that Shh-C199* retains the ability to induce the Hh response *in cis*. The mechanism by which Shh-E90A, -H183A and ShhN allow activation of the Hh pathway *in cis* appears to be related, as the double mutants (*ShhN-E90A* and *ShhN-H183A*) have the same activities as the single mutants (Figure 1A), and do not produce additive effects.

Together these results demonstrate that presumed loss-of-function mutations (Shh-H183A, Shh-E90A, Shh-C199S, ShhN-E90A, and ShhN-H183A), all have the ability to signal cell-autonomously

in cells lacking Ptch1/2 receptors. Cell-autonomous activation of the Hh response by Shh does not require processing of the pro-protein, nor binding to its (co-)receptors.

Shh mutants can activate the Hh response in the developing neural tube

To verify that Shh can activate the Hh pathway *in cis* independent of receptor function, we tested a variety of Shh mutants deficient in their ability interact with (co)-receptors in the developing neural tube. Along with Shh-E90A and Shh-H183A, we tested Shh-199A, a mutant form that cannot undergo autoproteolysis, and ShhN-C25S a mutant form lacking the N-terminal acyl group which has been shown to be unable to interact with Ptch1 (Tukachinsky et al., 2016). We assessed the activity of Shh mutants *in vivo* by co-electroporating *Shh*, *Shh-E90A, Shh-H183A*, or *Shh-199A*, together with *GFP* in developing chick neural tubes. Expression of Shh, Shh-E90A, and Shh-C199A caused an expansion of Nkx2.2 and Mnr2 domains, as well as repression of Pax7 expression (Figure 2, panels A-H), indicating that these forms of Shh are active, despite their inability to interact with canonical receptors. Electroporation of *Shh-H183A* does not result in activation of the pathway (Figure 2 C, G, K). However, we found that *ShhN-H183A* could induce the Hh response after electroporation (Figure 2 C',G',K'), thus indicating that correct Zn^{2+} coordination is not required to activate the Hh response *in vivo*. Consistent with the activity of *Shh-E90A*, we found that *ShhN-E90A* was active in this assay, as was *ShhN-C25S*. Altogether, the *in vivo* results support our findings *in vitro* demonstrating that the binding of Shh to Ptch1/2, Cdo, Boc or Gas1 is not necessary to activate the Hh response. They further demonstrate that Hh pathway activity is associated with the Shh pro-protein.

The canonical model implicates the loss of Ptch1-mediated inhibition of Smo as the central mechanism by which the Hh response is activated. The observation that the Hh pathway can be activated by Shh in the absence of Ptch1/2 function raises the question of whether or not this pathway activation is mediated by Smo.

***In cis* activation of the Hh response by ShhN requires Smo**

The *Ptch1/2* null fibroblast line used in this study is derived from *Ptch1*$^{LacZ/LacZ}$;*Ptch2*$^{-/-}$ mESCs (Roberts et al., 2016), which in turn are derived from *Ptch1*$^{LacZ/LacZ}$ mESCs (Goodrich et al., 1997); consequently, these cells carry the *Ptch1:LacZ* null allele. As *Ptch1* itself is invariably induced in cells responding to Shh, the *Ptch1:LacZ* allele has found widespread use as a dependable readout of Hh pathway activation. To further assess the nature of cell-autonomous pathway activation, we also used *Ptch1*$^{LacZ/LacZ}$ fibroblasts, used to study the of role of Ptch1 (Taipale et al., 2002), as a control. Transfection of *ShhN* into either cell line resulted in an activation of the transcriptional Hh response, i.e. a significant increase of transcriptional activity over the mock transfected cells. This activation could be blocked with the addition of vismodegib, a small molecule inhibitor of Smo (Sharpe et al.,

2015) (Figure 3A). The ability of vismodegib to block Ptch1/2-independent activation of the Hh response, as a consequence of *ShhN* expression, demonstrates that this activity is mediated by Smo. This experiment was repeated using the *Gli-Luciferase* reporter as an independent readout in four independent cell lines of varying genotypes. The *Gli-Luciferase* reporter was invariably induced upon transfection with *ShhN*, regardless of whether the cells were Ptch1/2 proficient, *Ptch1* null, or lacked both Ptch1 and Ptch2 function (Figure 3B). The resulting Hh pathway activation could be lowered by vismodegib in all cell lines, further demonstrating the involvement of Smo in cell-autonomous signaling. *Gli-Luciferase* induction after ShhN expression confirms the results obtained using the *Ptch1:LacZ* allele for quantification (Figure 3A). As shown before, *Ptch1*$^{LacZ/LacZ}$ fibroblasts have a moderate intrinsically upregulated Hh response after serum withdrawal (Taipale et al., 2002). This appears to be a unique characteristic of this particular cell line, as neither *Ptch1*$^{LacZ/LacZ}$;*Ptch2*$^{-/-}$ fibroblasts, nor *Ptch1*$^{-/-}$;*Disp1*$^{-/-}$;*Shh*$^{-/-}$ fibroblasts exhibit this property (Figure 3 B,D).

Cell-autonomous activation of the Hh response by *ShhN* in cells lacking Ptch1/2 activity could be inhibited by a dominant inhibitory form of Ptch1 and by the downstream transcription factor Gli3. Expression of *Ptch1ΔL2* (Briscoe et al., 2001) or *Gli3*^{PHS} (Meyer and Roelink, 2003) prevented upregulation of the Hh response by ShhN in both *Ptch1*$^{LacZ/LacZ}$ and *Ptch1*$^{LacZ/LacZ}$;*Ptch2*$^{-/-}$ cells (Figure 3C). Ptch1 catalytically acts upon Smo (Taipale et al., 2002), which in turn acts via the Gli transcription factors (Ruiz i Altaba, 1998; Stamataki et al., 2005), thus these results indicate that ShhN expression activates Smo downstream of Ptch1/2 function and upstream of Gli function.

The Cysteine Rich Domain of Smo is required for its activation of Shh

ShhN can act as a cellular chemoattractant (Angot et al., 2008; Bijlsma et al., 2007). The chemotactic response to Shh is directional and does not require *de novo* transcription or translation, nor does it require the function of Gli proteins (Bijlsma et al., 2007; 2008; Chinchilla et al., 2010; Lipinski et al., 2008). Chemotaxis towards Shh is mediated by Smo (Charron et al., 2003); however, it does not require the localization of Smo to the primary cilium, a prerequisite of the transcriptional response. Furthermore, chemotaxis can be mediated by forms of Smo unable to activate the transcriptional response to Shh (Bijlsma et al., 2012), indicating fundamental differences between these two activities of Smo. Translocation of Smo to the primary cilium involves Ptch1 function (Rohatgi et al., 2007), and we have previously shown that cells lacking *Ptch1* retain the ability to migrate towards ShhN (Alfaro et al., 2014b). Because Ptch1 and Ptch2 have overlapping functions (Alfaro et al., 2014b; Y. Lee et al., 2006; Roberts et al., 2016), it is not clear whether the chemotactic response in *Ptch1*$^{LacZ/LacZ}$ cells is mediated by Ptch2 or if it is a Ptch1/2-independent signaling event. We tested the ability of *Ptch1*$^{LacZ/LacZ}$;*Ptch2*$^{-/-}$ fibroblasts to migrate towards a localized source of ShhN using a

modified Boyden chamber (H. C. Chen, 2005). We found that *Ptch1*$^{LacZ/LacZ}$;*Ptch2*$^{-/-}$ cells were indistinguishable from *Ptch1*$^{LacZ/LacZ}$ cells in their ability to migrate towards ShhN (Figure 4A). Shh chemotaxis was largely abolished in *Ptch1*$^{LacZ/LacZ}$;*Ptch2*$^{-/-}$;*Smo*$^{-/-}$ cells; however, the ability to migrate towards FCS, our positive control, was retained (Figure 4A).

We could restore the ability of *Ptch1*$^{LacZ/LacZ}$;*Ptch2*$^{-/-}$;*Smo*$^{-/-}$ cells to migrate towards ShhN by transfecting them with wild type *Smo*, demonstrating the sufficiency of Smo to mediate Shh chemotaxis independent of Ptch1/2 function. (Figure 4A). However, transfection of a form of Smo lacking its CRD (*Smo-ΔCRD*) did not restore the chemotactic response in *Ptch1*$^{LacZ/LacZ}$;*Ptch2*$^{-/-}$;*Smo*$^{-/-}$ cells. These results demonstrate that Smo can recognize ShhN in the extracellular space to mediate the chemotactic response in the absence of Ptch1/2, and the CRD of Smo is required for this signaling event.

We used a *Smo*$^{-/-}$ fibroblast cell in lieu of the *Ptch1*$^{LacZ/LacZ}$;*Ptch2*$^{-/-}$;*Smo*$^{-/-}$ cell line to assess the requirement of the CRD of Smo to mediate the cell-autonomous transcriptional response. This was necessitated by our experience that *Ptch1*$^{LacZ/LacZ}$;*Ptch2*$^{-/-}$;*Smo*$^{-/-}$ cells do not survive the four days of serum deprivation necessary for the transcriptional assays. To ensure that we strictly measured cell-autonomous Ptch1/2-independent signaling, we used the *Shh-E90A* and *Shh-H183A* mutants that cannot signal non-cell autonomously. As expected, transfection of either *Shh-H183A* or *Shh-E90A* alone in *Smo*$^{-/-}$ cells did not result in the induction of the Hh response (Figure 4C). Transfection of *Smo* or *Smo-ΔCRD* alone caused a small upregulation of the Hh response. Consistent with earlier results (Figure 1A), we found that co-transfection of *Shh-E90A* or *Shh-H183A* together with *Smo* caused a strong induction of the Hh response *in cis.* In contrast, neither Shh-H183A nor Shh-E90A was capable of synergizing with Smo-ΔCRD to induce the Hh response, further demonstrating that the activation of Smo by Shh requires the CRD of Smo.

Despite its inability to respond to Shh, Smo-ΔCRD remains subject to inhibition by Ptch1. Mis-expression of *Smo-ΔCRD* in the developing chick neural tube after electroporation causes an upregulation of the Hh response (Figure 4D), consistent with earlier reports that Smo-ΔCRD retains a relatively high level of basal activity in vivo (Kwong et al., 2014). The activity of Smo-ΔCRD was suppressed by co-expression of *Ptch1ΔL2*, coding for a dominant-inhibitory form of Ptch1 (Briscoe et al., 2001) (Figure 4D). Similarly, expression of either *Smo* or *Smo-ΔCRD* in *Ptch1*$^{LacZ/LacZ}$;*Ptch2*$^{-/-}$ cells results in transcriptional Hh activity, which can be inhibited by co-expression with *Ptch1* or *Ptch1ΔL2* (Figure 4E). Together these results that the CRD of Smo is required for its activation by ShhN, but not for its repression by Ptch1.

The "pseudo-active" site of Shh has a role in Shh function other than receptor binding

Shh-E90 and -H183 are involved in the binding of Ca^{2+} and Zn^{2+} metal ions, respectively, and the coordination of the Zn^{2+} ion by H141, D148, and H183 (the "triad", Figure 6A) resembles that of Zn^{2+} peptidases, (Hall et al., 1995a) including Thermolysin (Rebollido-Rios et al., 2014). Hhs belong to a larger family of DD-transpeptidases (van Heijenoort, 2011) that has many members in prokaryotes. In general, such carboxypeptidases resolve the acyl-enzyme intermediate with a nucleophile other than OH^-, resulting in a sidechain addition (Fonzé et al., 1999). Peptidase activity of Shh is not required for activation of the Hh response (Fuse et al., 1999), (Figure 1 A, Figure 2), and the Zn2+ coordination was therefore often referred to as a "pseudo-active" site (Bosanac et al., 2009; Maun et al., 2010).

Figure 1B shows that Shh-H183A does not undergo autoproteolytic processing. To assess if the Zn^{2+} coordination triad is required for the formation of $ShhN_{Chol}$ we also made Shh-H141A and Shh-D148A, and confirming earlier observations on SHH-H140P (Traiffort et al., 2004), we found that Shh-H141D did not auto-process, and D148A processed very poorly (Figure 5A). Together, this shows that correct Zn^{2+} coordination is necessary for processing the Shh pro-protein into $ShhN_{Chol}$.

In Zn^{2+} peptidases, the E177 equivalent abstracts a proton from the catalytic water at the Zn^{2+} coordination domain, which is followed by a nucleophilic attack of the OH^- on the peptide backbone. Shh-E177A is, therefore, predicted to lack the intrinsic peptidase activity. Published analysis of this mutant has revealed two interesting properties. First, Shh-E177A is unable to mediate Shh signaling from the notochord to the overlying neural tube (*in trans*), but is more capable than wt Shh to induce the Hh response when expressed in the developing neural tube (likely *in cis*) (Himmelstein et al., 2017). Second, ShhN-E177A is more stable in solution than ShhN (Rebollido-Rios et al., 2014). We found that the Shh-E177A pro-protein was processed normally (not shown). Thus although the Zn^{2+} triad is required for processing of the Shh pro-protein, this does not appear to proceed via a canonical intrinsic peptidase activity. This is further supported by our finding that after co-expressing the obligatory pro-proteins Shh-C199A (unable to be cleaved) and Shh-H183A (unable to cleave) we could not detect any $ShhN_{Chol}$ (not shown).

Both H141 and D148 are found mutated in holoprosencephaly, a congenital syndrome that can be caused by aberrant SHH signaling (Hehr et al., 2010; Odent et al., 1999; Roessler et al., 2009). It was observed before that several holoprosencephaly mutants prevent processing of the SHH pro-protein (Traiffort et al., 2004), indicating that the perdurance of the SHH pro-protein might contribute to this congenital syndrome. As we found that the obligatory Shh pro-protein (Shh-C199A) was able to induce the Hh response in vivo we tested if failure of Shh processing could alter the Hh response.

The autocatalytic processing of the Shh pro-protein is relatively slow, and to minimize potential overexpression artefacts we tested Shh expressed using the human *Elongation Factor 1α* (*EF1α*) promoter, which is much weaker than the *CMV* promoter used in previous experiments. When driven by the *EF1α* promoter, we found very little activity associated with Shh, unlike *Shh* driven by the *CMV* promoter (Figure 5C). Analysis of the protein expressed in these transfected cells (Figure 5B) revealed that the amount of observed Shh pro-protein correlates with the level of Hh pathway induction; this is in contrast to the amount of observed $ShhN_{Chol}$, which was not correlated with pathway activity (Figure 5C,D). These observations further advance the notion that $ShhN_{Chol}$ is unable to induce the Hh response *in cis* and that the Shh pro-protein can activate the Hh response.

The low level of Hh pathway induction observed in cells expressing *EF1α*-driven *Shh* allowed us to assess if Shh mutations result in a gain-of-function phenotype, as measured by activation of the transcriptional Hh response *in cis*. We tested mutations affecting the Zn^{2+} coordination domain, the Ca^{2+} coordination domain, mutations affecting the putative peptidase activity, and a series of holoprosencephaly mutants, in particular those in the large α-helix that dominates the face of Shh opposite to the Zn^{2+} coordination domain, and some mutations (W118R/G and C184F) tested (Traiffort et al., 2004). All these mutants were directly introduced into the *Shh* clone that had little activity after transfection. We found that Zn^{2+} coordination triad mutants (D148N, and H183A, blue bars, Figure 5E), caused no or minimal activation of the Hh response as compared to wild-type Shh. In contrast, E90A and H135A gained the ability to induce Hh response *in cis*, while being processed normally. Traiffort demonstrated that W118R/G does not process (Traiffort et al., 2004). Tryptophan118 is at the C-terminal end of the large α-helix. This helix is enriched in mutations found in holoprosencephaly patients (Figure 6C), and we tested Q101H, C103Y/R, A111D/Y I112F/N, N116L and W118R/G. All these of Shh point mutations are gain-of-function mutants in their ability to induce the Hh response *in cis*. This activation does not require processing of the Shh pro-protein, as a majority of the tested holoprosencephaly mutants in the large α-helix do not give rise to $ShhN_{Chol}$ (Figure 5F). This suggests that at least some cases of holoprosencephaly are caused by the acquisition of cell autonomous, Ptch1/2-independent Hh signaling via the SHH pro-protein, while leaving non-autonomous signaling via the wild type allele intact.

Discussion

Ptch1/2-independent activation of Smo by Shh

Our observations challenge the canonical model that Smo activation is solely mediated by the Shh-induced release of Ptch1 inhibition. Despite the ample evidence that Ptch1 is an efficient inhibitor of Smo (Goodrich et al., 1997), we find that: 1) the loss of *Ptch1/2* does not inevitably result in maximal

Smo activation, and 2) several forms of Shh can activate the migrational and transcriptional Hh responses in the absence of Ptch1/2 function. Nevertheless, Ptch1 function is required in those same cells to transcriptionally respond to ShhN provided extracellularly (Roberts et al., 2016). A central role of Ptch1 function is to regulate Smo entry into the primary cilium (Rohatgi et al., 2007), which is required for the transcriptional Hh response (Goetz and Anderson, 2010) but dispensable for the chemotactic response (Bijlsma et al., 2012). Our observations are consistent with a model in which Shh can both bind to Ptch1/2 (Rohatgi et al., 2007), resulting in the localization of Smo to the primary cilium where it mediates the transcriptional response, and activate Smo independent of Ptch1/2 function, resulting in fast changes in cell shape that underlie chemotaxis. This model would require the function of Ptch1/2 to couple extracellular Shh to the Gli-mediated transcriptional response, something that might be circumvented by some of Shh mutants we described.

Whether cells lacking Ptch1 or Ptch2 retain sensitivity to Shh *in vivo* is unclear. However, some observations indicate that they might. The spectrum of tumors observed in *Ptch1* null and in *Ptch1/2* heterozygous mice (Y. Lee et al., 2006) are commonly found at sites where Shh is expressed; and Shh-induced tumors often arise at the same locations (Beachy et al., 2004). The positional overlap between tumors induced by the loss of Ptch function and Shh-induced tumors is compatible with our model that cells lacking Ptch1/2 function nevertheless retain some ability to respond to Shh. Our model is further supported by the observation that the establishment of left/right asymmetry in mouse embryos, determined by *Pitx2* expression, requires *Smo*, *Shh*, and *Ihh*, but not *Ptch1* (X. M. Zhang et al., 2001). *Ptch1*$^{-/-}$ mutant embryos establish normal asymmetric expression of *Pitx2*, indicating that this Hh/Smo-mediated symmetry-breaking event occurs independently of Ptch1. Furthermore, the upregulation of pathway activity observed in *Ptch1*$^{LacZ/LacZ}$ mice coincides with a widespread expression of Shh in the developing neural tube, leaving open the possibility that this activation remains Shh-dependent.

The ability of Shh to activate Smo in a relatively direct manner is supported by the observations that ShhN activates the Hh pathway in cells lacking all known extracellular receptors and that forms of Shh unable to bind to these receptors activate the pathway in a Smo-dependent manner. Furthermore, we demonstrate that the CRD of Smo is required for both Shh-mediated transcriptional and migrational responses. The idea that the CRD of Smo is a target of Shh-mediated activation is supported by the previous observations that Smo-ΔCRD has a decreased sensitivity to Shh *in vitro* and *in vivo* (Aanstad et al., 2009; Myers et al., 2013; Nachtergaele et al., 2013). The regulation of Smo facilitated by Ptch1/2-mediated inhibition likely targets the heptahelical domain of Smo, a notion that has previously been suggested based on the action of many small molecule Smo inhibitors, such as Cyclopamine (J. K. Chen et al., 2002) and vismodegib (Byrne et al., 2016). This indicates

that the mechanism by which Smo is inhibited and activated are not the same, consistent with the findings that: 1) Ptch1 can inhibit forms of Smo lacking the CRD (Myers et al., 2013), and 2) the binding of oxysterols and cholesterol to the CRD can activate Smo (Huang et al., 2016; Nachtergaele et al., 2013; 2012; Nedelcu et al., 2013).

Shh autoproteolysis is not required for Smo activation

Our results demonstrate that a wide variety of Shh mutants, several previously characterized as "dead", have the ability to activate Smo *in cis* when expressed in cells lacking the canonical receptors in vitro and in wild-type cells in vivo. ShhC199A, which remains unprocessed as a full length precursor poorly signals *in trans* (Pettigrew et al., 2014; Roelink et al., 1995), but can induce the Hh response *in cis*. Several Shh mutations cause persistence of the pro-proteins (C103Y/R, A111D/Y I112F/N, N116L, W118R/G, and C184Y) and these mutants can activate Hh response *in cis*. These results indicate that one important function of the unusual processing and modification of Shh is to prevent activation of the Hh response in cells that express the ligand, thus reinforcing strict non-cell autonomy that characterizes Shh signaling (García-Zaragoza et al., 2012; Shaw et al., 2009; Yauch et al., 2008).

The Zn^{2+} coordination site is involved in the binding to Hhip (Bosanac et al., 2009) 5E1 (Maun et al., 2010) and possibly Ptch1. The resemblance to the active site of Zn^{2+} peptidases was recognized early (Hall et al., 1995b), and this site was thought be not catalytically active, but instead was proposed to mediate binding to Ptch1 (Fuse et al., 1999). The Zn^{2+} coordination domain is required for autoproteolytic processing, consistent with the notion that (similar to Thermolysin), the Zn^{2+} triad is catalytically active. At low expression levels the Zn^{2+} triad mutants are poor inducers of the Hh response at best. However, several other mutants outside the triad prevent autoproteolytic processing, and gain the ability to induce the Hh response *in cis*. This indicates that the Zn^{2+} coordination domain, even in the pro-protein, appears to be involved in the activation of the Hh response in cells lacking Ptch1/2, and might thus be involved in the Ptch1/2-independent activation of Smo.

The ShhN domain, the mature signaling peptide that contains the Zn^{2}coordination site, has highly conserved homologs in bacteria (Accession numbers in the Materials and Methods). Identitcal encompasses all critical amino acids involved in metal coordination, identical residues between Hh found in *Rhizobium* and mouse/human are indicated in Figure 6C. These predicted bacterial Hh proteins are members of a larger group of prokaryotic peptidases that are characterized by the Hedgehog/DD-transpeptidase motif (van Heijenoort, 2011). The signature transpeptidase domain is a central, five-stranded antiparallel β-sheet surrounded by α-helices, as found in ShhN. Members of

this family include murein endopeptidase (penicillin resistant enzymes that modify bacterial cell walls) and peptidase M15 (bacterial D-alanyl-D-alanine carboxypeptidases (DD-transpeptidases), the target for penicillin). Like in Shh, in all DD-transpeptidases Zn^{2+} is coordinated by two Histidine residues and an Aspartic acid residue in a H-X(6)-D and H-X-H motif (H141 D148, H181, H183 for Shh). DD-transpeptidases use a catalytic mechanism in which the acyl-linked peptide-enzyme intermediate is resolved by a nucleophilic attack of the adjacent peptidoglycan chain, thus cross-linking the peptidoglycan chains in the bacterial cell wall. This mechanism is possibly related to resolving the reaction intermediate that exists during Shh autocleavage by cholesterol nucleophilic attack, resulting in $ShhN_{Chol}$. It is thus possible that the Hh/DD-transpeptidase fold has evolved to prevent resolution of the peptide-enzyme intermediate by OH^-, resulting in proteolysis.

This model is not consistent with the one proposed by the Beachy lab that requires C199 to allow a thiol-ester intermediate to be resolved by cholesterol (Porter et al., 1996). Our observation that C199S undergoes some processing (Figure 5E) cannot be explained by the Beachy model, but is consistent with a function of Shh as auto-transpeptidase that auto-processes.

Shh mutants found in tumors and in individuals with holoprosencephaly

It is striking that several mutations found in SHH-induced Basal Cell Carcinomas (BCCs) (Couvé-Privat et al., 2004) (SHH-D147N and SHH-R155C) are defective in auto-processing (Figure 5 and not shown). It is unlikely that these mutations are inhibitory to Hh signaling and consistent with the idea that such mutants are gain-of-function as measured by the cell-autonomous activation of the Hh response. SHH Point mutations curated in the COSMIC database tend to be more prevalent in the SHHN domain, but are common in the SHHC domain right after the cleavage site. Asymmetric distribution indicates that at least some of the mutations are ”drivers” in tumor formation. Several of the N-domain mutations involve residues that activate the cell autonomous response when mutated (E89K, H134Q, and C183Y). Several point mutations in gall bladder tumors are found in SHHC (Dixit et al., 2017), and at least one of these (Shh-K213E) fails to process. These findings are consistent with a model in which SHH mutations permit *in cis* activation of the Hh response, thereby contributing to tumor progression.

In humans, heterozygous *SHH* mutants causing single amino acid substitutions can cause holoprosencephaly (Hehr et al., 2010), although mice heterozygous for a null *Shh* allele are normal. It is thus possible that some of these point mutations are dominant-negatives or gain-of-function mutations. The analysis of point mutations that cause holoprosencephaly (Roessler et al., 2009) reveal an interesting pattern. Residues involved the Zn^{2+} coordination, and thus likely required for the peptidase activity, are targets for point mutations in holoprosencephaly (H140, and D147, human

numbering), but also heterozygous mutations in the C-terminal domain of SHH can cause holoprosencephaly (Hehr et al., 2010). Mutations in the C-terminal domain likely interfere with auto-processing of full length Shh and cholesterol addition to G197 of SHH. It is thus possible that either unprocessed SHH or SHH lacking the putative peptidase activity function as a dominant-negative forms of Shh as proposed by Singh *et al.* (Singh et al., 2009). Alternatively, a cell-autonomous activation of the Hh response (a gain-of-function mutation) in cells heterozygous for this mutation could contribute to holoprosencephaly. We think the latter explanation is more plausible given the gain-of-function phenotypes we find associated with *Shh* mutants that fail to process, or lack the cholesterol moiety.

Model

Based on our results in cells lacking Ptch1/2 and those of others, we propose the following model to account for the strict non-cell autonomy of Shh signaling (Figure 6 D). Although the Shh pro-protein has the ability to activate the Hh response, this is prevented by the processing into the inactive $ShhN_{Chol}$ form. This form is activated upon Disp1, Scube2, and metalloproteases to be released in an active form (Jakobs et al., 2014) that signals *in trans*. Mutations that prevent efficient processing of the Shh pro-protein, or prevent the addition of the cholesterol moiety allow cell autonomous activation of the Hh response. The activation of this response does not require, but likely is antagonized by Ptch1/2, It does, however, require the CRD of Smo, perhaps indicating that Smo is a receptor for Shh.

Materials and Methods

Materials: Vismodegib was a gift from Dr. Fred de Sauvage (Genentech). SAG was from EMD Biochemicals. Recombinant ShhN protein was from R&D Systems. Cell Tracker Green CMFDA was from Invitrogen.

Electroporations: Hamburger-Hamilton (HH) stage 10 *Gallus gallus* embryos were electroporated caudally in the developing neural tube using standard procedures (Meyer and Roelink, 2003). Embryos were incubated for another 48 h following electroporation, dissected, fixed in 4% PFA, mounted in Tissue-Tek OCT Compound (Sakura) and sectioned.

Embryoid Body differentiation: mESCs were neuralized and differentiated into embryoid bodies (NEBs) using established procedures (Wichterle et al., 2002). NEBs were harvested after 5 days in culture, fixed, and stained for Nkx2.2 and Isl1/2 (Kawakami et al., 1997). NEBs were mounted in Fluoromount-G (Southern Biotech) and imaged.

Immunofluorescence: Antibodies for mouse Pax7 (1:10), Mnr2 (1:100), Nkx2.2 (1:10), Shh (5E1, 1:20) were from the Developmental Studies Hybridoma Bank. The Rabbit α-GFP (1:1000) antibody was from Invitrogen, and the Goat α-hOlig2 (1:100) antibody was from R&D Systems. The mouse α-acetylated tubulin (1:200) was from Sigma Aldrich. Alexa488 and Alexa568 secondary antibodies (1:1000) were from Invitrogen. Nuclei were stained with DAPI (Invitrogen).

DNA Constructs: The *Gli-Luciferase* reporter and the Renilla control were gifts from Dr. H. Sasaki (Sasaki et al., 1997). *Ptch1* was a gift from Dr. Scott (Stanford University, CA, USA). *Ptch1-Δloop2* was a gift from Dr. Thomas Jessell (Columbia University, NY, USA). *Ptch1* channel mutants were previously described (Alfaro et al., 2014a). SmoΔCRD was a gift from J. Reiter (Aanstad et. al., 2009). SmoM2 was from Genentech (F. de Sauvage). The following mutations were created using Quikchange mutagenesis (Stratagene): *Shh-E90A*, *Shh-H183A*, *ShhN-E90A*, *ShhN-H183A*, *SmoΔCRD-CLD*, *SmoL112DW113Y.* Dhh and Ihh were gifts from Charles Emerson Jr. (University of Massachusetts Medical School, MA, USA). *DhhN* and *IhhN* were made by site directed mutagenesis of C199 (Dhh) and C203 (Ihh) to a stop codon. ShhC199A was previously described (Roelink et al., 1995). $Gli3^{PHS}$ was previously described (Meyer et. al., 2003).

Genome Editing: TALEN constructs targeting the first exon of mouse Cdo and Gas1 were designed and cloned into the pCTIG expression vectors containing IRES puromycin and IRES hygromycin selectable markers (Cermak et al., 2011). The following repeat variable domain sequences were generated: Cdo, 5' TALEN: NN HD NI NG HD HD NI NN NI HD HD NG HD NN NN ; 3' TALEN: HD NI HD NI NI NN NI NI HD NI NG NI HD NI NN; Gas1, 5' TALEN: NN NI NN NN NI HD NN HD HD HD NI NG NN HD HD; 3' TALEN: NN NN NI NI NI NI NN NG NG NG NN NG HD HD NN NI. Two CRISPR constructs targeting a double strand break flanking the first exon of mouse Boc were cloned into *pSpCas9* vector with an IRES puromycin selectable marker (Ran et al., 2013). The Boc CRISPRs targeted the following forward genomic sequences (PAM sequences underlined): Upstream of first exon 5' CCTGTCCTCGCTGTTGGTCCCTA 3'; Downstream of first exon 5' CCCACAGACTCGCTGAAGAGCTC 3'. $Ptch1^{LacZ/LacZ}$;$Ptch2^{-/-}$;$Shh^{-/-}$ mouse embryonic stem cells (Roberts et al., 2016) were plated at a density of 1.0×10^6 on 6-well plates and transfected with 6 genome editing plasmids the following day. One day after transfection, selective ES medium (100 µg/mL hygromycin and 0.5 µg/mL puromycin) was added for 4 days. Selective medium was removed and surviving mESC colonies were isolated, expanded and genotyped by sequence PCR products spanning TALEN and CRISPR-binding sites.

Genotyping: PCR screening was performed on cell lysates using primers flanking the TALEN or CRISPR binding sites for the *Boc*, *Cdo*, and *Gas1* loci. *Boc*, (5')

CATCTAACAGCGTTGTCCAACAATG and (3') CAAGGTGGTATTGTCCGGATC; *Cdo*, (5') CACTTCAGTGTGATCTCCAG and (3') CCTTGAACTCACAGAGATTCG; Gas1, (5') ATGCCAGAGCTGCGAAGTGCTA and (3') AGCGCCTGCCAGCAGATGAG. PCR products were sequenced. Samples with signals indicative of INDEL mutations were cloned into the pCR-BluntII vector using the Zero Blunt TOPO PCR cloning kit (Invitrogen) and sequenced to confirm allele sequences. A *Ptch1*$^{LacZ/LacZ}$;*Ptch2*$^{-/-}$;*Boc*$^{-/-}$;*Cdo*$^{-/-}$;*Gas1*$^{-/-}$;*Shh*$^{-/-}$ mESC clone was identified harboring a 50 bp deletion in Cdo exon 1, a heteroallelic 480 bp insertion and a 200 bp deletion in Gas1 exon1 resulting in a premature stop codon in the reading frame, and a 450 bp deletion of Boc exon 1.

Cell Culture: *Ptch1*$^{LacZ/LacZ}$;*Ptch2*$^{-/-}$, *Ptch1*$^{LacZ/LacZ}$;*Ptch2*$^{-/-}$;*Smo*$^{-/-}$, *Ptch1*$^{-/-}$;*Disp1*$^{-/-}$;*Shh*$^{-/-}$, and *Ptch1*$^{LacZ/LacZ}$;*Ptch2*$^{-/-}$;*Boc*$^{-/-}$;*Cdo*$^{-/-}$;*Gas1*$^{-/-}$;*Shh*$^{-/-}$ fibroblasts were obtained by plating mESCs at a density of 8.0×10^5 cells in 6-well plates and transfected with the *large T antigen* from the SV40 virus (Gökhan et al., 1998) in ES medium. Cells were then switched to DMEM (Invitrogen) supplemented with 10% fetal bovine serum (FBS) without LIF. *Ptch1*$^{+/LacZ}$ and *Ptch1*$^{LacZ/LacZ}$ fibroblasts (gifts from Dr. Scott) were cultured in DMEM supplemented with 10% FBS (Invitrogen) and maintained under standard conditions. Identity of these lines was confirmed by the presence of the LacZ recombination in the Ptch1 locus, the presence of 40 chromosomes per cell, and mouse-specific DNA sequences of the edited genes. mESC lines were maintained using standard conditions in dishes coated with gelatin, without feeder cells. Cells were routinely tested for Mycoplasm by Hoechst stain, and grown in the presence of tetracycline and gentamycin at regular intervals. Cultures with visible extranuclear staining, likely infected with Mycoplasma, were discarded. None of the cell lines used in this study is listed in the Database of Cross-Contaminated or Misidentified Cell Lines. Fibroblast-like lines derived from the mESCs were re-sequenced at the edited loci to confirm their identity.

Transfection: Cells were transiently transfected for 24h at 80-90% confluency using Lipofectamine 2000 reagent (Invitrogen) according to the manufacturer's protocol.

Modified Boyden Chamber Migration Assay: Cell migration assays were performed as previously described (Bijlsma et. al. 2007). Cells were labeled with 10 µM CellTracker Green (Invitrogen) in DMEM for one hour. The well compartments were set up with the specified chemoattractant (ShhN .75 µg/ML (resuspended in 0.1%BSA in PBS), 10% FCS, or no attractant (plus 0.1%BSA in PBS) and pre-warmed at 37˚C. Cells were then detached with 5mM EDTA and resuspended in DMEM without phenol red and supplemented with 50mM HEPES. Cells were transferred into FluoroBlok Transwell inserts (BD Falcon) at 5.0×10^4 cells per insert. GFP-spectrum fluorescence in the bottom compartment was measured every 2 min for 99 cycles (approximately 3 hours), after which

background fluorescence (medium without cells) and a no-attractant control was subtracted from each time point. Starting points of migration were set to 0.

Gli-Luciferase Assay: Fibroblasts were plated at a density of $3x10^4$ in 24 well plates and transfected with *Gli-Luciferase*, *CMV-Renilla* (control plasmid), and specified plasmids 24 hours after plating. Cells were grown to confluency and then switched to low serum medium (0.5% FBS) alone or with specified concentrations of Vismodegib. After 24 hours, cells were lysed and the luciferase activity in lysates was measured using the Dual Luciferase Reporter Assay System (Promega). Raw Luciferase values were normalized against Renilla values for each biological replicate to control against variation in transfection efficiency. Individual luciferase/renilla values were then normalized against the mock control average for each experiment.

LacZ Assay: Fibroblasts were plated at a density of $3x10^4$ in 24 well plates and transfected with plasmids 24 hours after plating. Fibroblasts were grown to confluency and then switched to a low serum medium (0.5% FBS) alone or with specified concentrations of Vismodegib or SAG. After 24 hours, cells were lysed and lysates were analyzed using the Galacto-Light™ chemiluminescence kit (Applied Biosciences) for level of LacZ expression. Raw chemiluminescence values were normalized against total protein for each biological replicate. Protein concentration was determined with a Bradford assay using the Bio-Rad Protein Assay Dye Reagent.

Western Blots: *Ptch1*$^{LacZ/LacZ}$*;Ptch2*$^{-/-}$ cells were transfected with Shh mutants as indicated. 48 hours after transfection, *Ptch1*$^{LacZ/LacZ}$*;Ptch2*$^{-/-}$ cells were rinsed with PBS and lysed with RIPA buffer (150 mM NaCl, 50 mM Tris-HCl, 1% Igepal, 0.5% Sodium Deoxycholate, and protease inhibitors) for 30 min on ice. Protein lysate was cleared by centrifugation at 13,000g for 30 min at 4 °C. 20 µg of each sample was run on a 12% SDS-PAGE gel and transferred to a 0.45 micron nitrocellulose membrane. Membranes were blocked with 5% milk in Tris-buffered saline with 0.1% Tween-20 (TBS-T) and incubated with a rabbit polyclonal anti-Shh antibody (H160; Santa Cruz Biotechnology) at 1:250. A goat anti-rabbit HRP-conjugated secondary antibody (BioRad) was used at 1:10000.

NCBI Reference Sequence Mesorhizobium HhN: WP_029077494.1

Acknowledgements: This work was supported by NIH grant 1R01GM117090 to HR. Vismodegib was a gift from Dr. de Sauvage (Genentech), *Dhh* and *Ihh* were a gift from Dr. Charles P. Emerson III (U. Mass. Med. School). Dr. A. Alfaro cloned the Shh binding mutants (E90A, H183A) and made the initial observation that they activate the Hh pathway *in vivo*. We thank Dr. M. Barro for her help with Western blotting, Dr. M. F. Bijlsma (AMC Amsterdam) for his help with the migration assays, and Dr. B. Roberts (Allen Institute for Cell Science) for his comments and advice. We also thank Fatma Ozguc for help with genome editing of the *Ptch1*$^{LacZ/LacZ}$;*Ptch2*$^{-/-}$;*Boc*$^{-/-}$;*Cdo*$^{-/-}$;*Gas1*$^{-/-}$;*Shh*$^{-/-}$ mESC line and Michelle Boisvert for her help with generating Shh mutants, and Carina Jägers and Wei Lu for commenting on the manuscript.

Author contributions: CC performed nearly all experiments. HR and CC designed the experiments and wrote the manuscript.

References

Aanstad, P., Santos, N., Corbit, K.C., Scherz, P.J., Trinh le, A., Salvenmoser, W., Huisken, J., Reiter, J.F., Stainier, D.Y., 2009. The extracellular domain of Smoothened regulates ciliary localization and is required for high-level Hh signaling. Curr. Biol. 19, 1034–1039.

Alfaro, A.C., Roberts, B., Kwong, L., Bijlsma, M.F., roelink, H., 2014a. Ptch2 mediates the Shh response in Ptch1-/- cells. Development (Cambridge, England). doi:10.1242/dev.110056

Alfaro, A.C., Roberts, B., Kwong, L., Bijlsma, M.F., roelink, H., 2014b. Ptch2 mediates the Shh response in Ptch1-/- cells. Development (Cambridge, England) 141, 3331–3339. doi:10.1242/dev.110056

Allen, B.L., Song, J.Y., Izzi, L., Althaus, I.W., Kang, J.S., Charron, F., Krauss, R.S., McMahon, A.P., 2011. Overlapping roles and collective requirement for the coreceptors GAS1, CDO, and BOC in SHH pathway function. Developmental cell 20, 775–787. doi:10.1016/j.devcel.2011.04.018

Angot, E., Loulier, K., Nguyen-Ba-Charvet, K.T., Gadeau, A.P., Ruat, M., Traiffort, E., 2008. Chemoattractive activity of sonic hedgehog in the adult subventricular zone modulates the number of neural precursors reaching the olfactory bulb. Stem cells (Dayton, Ohio) 26, 2311–2320.

Bale, A.E., 2002. Hedgehog signaling and human disease. Annu Rev Genomics Hum Genet 3, 47–65. doi:10.1146/annurev.genom.3.022502.103031

Beachy, P.A., Karhadkar, S.S., Berman, D.M., 2004. Tissue repair and stem cell renewal in carcinogenesis. Nature 432, 324–331. doi:10.1038/nature03100

Bhanot, P., Brink, M., Samos, C.H., Hsieh, J.C., Wang, Y., Macke, J.P., Andrew, D., Nathans, J., Nusse, R., 1996. A new member of the frizzled family from Drosophila functions as a Wingless receptor. Nature 382, 225–230.

Bijlsma, M.F., Borensztajn, K.S., Roelink, H., Peppelenbosch, M.P., Spek, C.A., 2007. Sonic hedgehog induces transcription-independent cytoskeletal rearrangement and migration regulated by arachidonate metabolites. Cellular signalling 19, 2596–2604.

Bijlsma, M.F., Damhofer, H., roelink, H., 2012. Hedgehog-stimulated chemotaxis is mediated by smoothened located outside the primary cilium. Sci Signal 5, ra60. doi:10.1126/scisignal.2002798

Bijlsma, M.F., Peppelenbosch, M.P., Spek, C.A., Roelink, H., 2008. Leukotriene synthesis is required for hedgehog-dependent neurite projection in neuralized embryoid bodies but not for motor neuron differentiation. Stem cells (Dayton, Ohio) 26, 1138–1145.

Bosanac, I., Maun, H.R., Scales, S.J., Wen, X., Lingel, A., Bazan, J.F., de Sauvage, F.J., Hymowitz, S.G., Lazarus, R.A., 2009. The structure of SHH in complex with HHIP reveals a recognition role for the Shh pseudo active site in signaling. Nature structural & molecular biology 16, 691–697.

Briscoe, J., Chen, Y., Jessell, T.M., Struhl, G., 2001. A hedgehog-insensitive form of patched provides evidence for direct long-range morphogen activity of sonic hedgehog in the neural tube. Molecular cell 7, 1279–1291.

Buglino, J.A., Resh, M.D., 2008. Hhat is a palmitoylacyltransferase with specificity for N-palmitoylation of Sonic Hedgehog. The Journal of biological chemistry 283, 22076–22088.

Byrne, E.F.X., Sircar, R., Miller, P.S., Hedger, G., Luchetti, G., Nachtergaele, S., Tully, M.D., Mydock-McGrane, L., Covey, D.F., Rambo, R.P., Sansom, M.S.P., Newstead, S., Rohatgi, R., Siebold, C., 2016. Structural basis of Smoothened regulation by its extracellular domains. Nature 535, 517–522. doi:10.1038/nature18934

Cermak, T., Doyle, E.L., Christian, M., Wang, L., Zhang, Y., Schmidt, C., Baller, J.A., Somia, N.V., Bogdanove, A.J., Voytas, D.F., 2011. Efficient design and assembly of custom TALEN and other TAL effector-based constructs for DNA targeting. Nucleic Acids Res. 39, e82. doi:10.1093/nar/gkr218

Charron, F., Stein, E., Jeong, J., McMahon, A.P., Tessier-Lavigne, M., 2003. The morphogen sonic

hedgehog is an axonal chemoattractant that collaborates with netrin-1 in midline axon guidance. Cell 113, 11–23.
Chen, H.C., 2005. Boyden chamber assay. Methods in molecular biology (Clifton, N.J 294, 15–22.
Chen, J.K., Taipale, J., Cooper, M.K., Beachy, P.A., 2002. Inhibition of Hedgehog signaling by direct binding of cyclopamine to Smoothened. Genes & development 16, 2743–2748.
Chinchilla, P., Xiao, L., Kazanietz, M.G., Riobo, N.A., 2010. Hedgehog proteins activate pro-angiogenic responses in endothelial cells through non-canonical signaling pathways. Cell cycle (Georgetown, Tex 9, 570–579.
Corcoran, R.B., Scott, M.P., 2006. Oxysterols stimulate Sonic hedgehog signal transduction and proliferation of medulloblastoma cells. Proceedings of the National Academy of Sciences of the United States of America 103, 8408–8413.
Couvé-Privat, S., Le Bret, M., Traiffort, E., Queille, S., Coulombe, J., Bouadjar, B., Avril, M.F., Ruat, M., Sarasin, A., Daya-Grosjean, L., 2004. Functional analysis of novel sonic hedgehog gene mutations identified in basal cell carcinomas from xeroderma pigmentosum patients. Cancer research 64, 3559–3565. doi:10.1158/0008-5472.CAN-03-4040
Dixit, R., Pandey, M., Tripathi, S.K., Dwivedi, A.N.D., Shukla, V.K., 2017. Comparative Analysis of Mutational Profile of Sonic hedgehog Gene in Gallbladder Cancer. Dig. Dis. Sci. 62, 708–714. doi:10.1007/s10620-016-4438-1
Fonzé, E., Vermeire, M., Nguyen-Distèche, M., Brasseur, R., Charlier, P., 1999. The crystal structure of a penicilloyl-serine transferase of intermediate penicillin sensitivity. The DD-transpeptidase of streptomyces K15. J. Biol. Chem. 274, 21853–21860.
Fuse, N., Maiti, T., Wang, B., Porter, J.A., Hall, T.M., Leahy, D.J., Beachy, P.A., 1999. Sonic hedgehog protein signals not as a hydrolytic enzyme but as an apparent ligand for patched. Proc. Natl. Acad. Sci. U.S.A. 96, 10992–10999.
García-Zaragoza, E., Pérez-Tavarez, R., Ballester, A., Lafarga, V., Jiménez-Reinoso, A., Ramírez, A., Murillas, R., Gallego, M.I., 2012. Intraepithelial paracrine Hedgehog signaling induces the expansion of ciliated cells that express diverse progenitor cell markers in the basal epithelium of the mouse mammary gland. Developmental biology 372, 28–44. doi:10.1016/j.ydbio.2012.09.005
Goetz, S.C., Anderson, K.V., 2010. The primary cilium: a signalling centre during vertebrate development. Nat. Rev. Genet. 11, 331–344. doi:10.1038/nrg2774
Goodrich, L.V., Milenkovic, L., Higgins, K.M., Scott, M.P., 1997. Altered neural cell fates and medulloblastoma in mouse patched mutants. Science (New York, N.Y 277, 1109–1113.
Gökhan, S., Song, Q., Mehler, M.F., 1998. Generation and regulation of developing immortalized neural cell lines. Methods 16, 345–358. doi:10.1006/meth.1998.0689
Hall, T.M., Porter, J.A., Beachy, P.A., Leahy, D.J., 1995a. A potential catalytic site revealed by the 1.7-A crystal structure of the amino-terminal signalling domain of Sonic hedgehog. Nature 378, 212–216.
Hall, T.M., Porter, J.A., Beachy, P.A., Leahy, D.J., 1995b. A potential catalytic site revealed by the 1.7-A crystal structure of the amino-terminal signalling domain of Sonic hedgehog. Nature 378, 212–216. doi:10.1038/378212a0
Hehr, U., Pineda-Alvarez, D.E., Uyanik, G., Hu, P., Zhou, N., Hehr, A., Schell-Apacik, C., Altus, C., Daumer-Haas, C., Meiner, A., Steuernagel, P., Roessler, E., Winkler, J., Muenke, M., 2010. Heterozygous mutations in SIX3 and SHH are associated with schizencephaly and further expand the clinical spectrum of holoprosencephaly. Hum. Genet. 127, 555–561. doi:10.1007/s00439-010-0797-4
Himmelstein, D.S., Cajigas, I., Bi, C., Clark, B.S., Van Der Voort, G., Kohtz, J.D., 2017. SHH E176/E177-Zn(2+) conformation is required for signaling at endogenous sites. Developmental biology 424, 221–235. doi:10.1016/j.ydbio.2017.02.006
Huang, P., Nedelcu, D., Watanabe, M., Jao, C., Kim, Y., Liu, J., Salic, A., 2016. Cellular Cholesterol Directly Activates Smoothened in Hedgehog Signaling. Cell 166, 1176–1187.e14. doi:10.1016/j.cell.2016.08.003

Incardona, J.P., Gruenberg, J., Roelink, H., 2002. Sonic hedgehog induces the segregation of patched and smoothened in endosomes. Curr. Biol. 12, 983–995.
Incardona, J.P., Lee, J.H., Robertson, C.P., Enga, K., Kapur, R.P., Roelink, H., 2000. Receptor-mediated endocytosis of soluble and membrane-tethered Sonic hedgehog by Patched-1. Proc. Natl. Acad. Sci. U.S.A. 97, 12044–12049. doi:10.1073/pnas.220251997
Izzi, L., Lévesque, M., Morin, S., Laniel, D., Wilkes, B.C., Mille, F., Krauss, R.S., McMahon, A.P., Allen, B.L., Charron, F., 2011. Boc and Gas1 each form distinct Shh receptor complexes with Ptch1 and are required for Shh-mediated cell proliferation. Developmental cell 20, 788–801. doi:10.1016/j.devcel.2011.04.017
Jakobs, P., Exner, S., Schürmann, S., Pickhinke, U., Bandari, S., Ortmann, C., Kupich, S., Schulz, P., Hansen, U., Seidler, D.G., Grobe, K., 2014. Scube2 enhances proteolytic Shh processing from the surface of Shh-producing cells. Journal of Cell Science 127, 1726–1737. doi:10.1242/jcs.137695
Janda, C.Y., Waghray, D., Levin, A.M., Thomas, C., Garcia, K.C., 2012. Structural basis of Wnt recognition by Frizzled. Science (New York, N.Y 337, 59–64. doi:10.1126/science.1222879
Kawakami, A., Kimura Kawakami, M., Nomura, T., Fujisawa, H., 1997. Distributions of PAX6 and PAX7 proteins suggest their involvement in both early and late phases of chick brain development. Mechanisms of development 66, 119–130.
Kristiansen, K., 2004. Molecular mechanisms of ligand binding, signaling, and regulation within the superfamily of G-protein-coupled receptors: molecular modeling and mutagenesis approaches to receptor structure and function. Pharmacol Ther 103, 21–80.
Kwong, L., Bijlsma, M.F., Roelink, H., 2014. Shh-mediated degradation of Hhip allows cell autonomous and non-cell autonomous Shh signalling. Nat Commun 5, 4849. doi:10.1038/ncomms5849
Lee, J.J., Ekker, S.C., von, K.D., Porter, J.A., Sun, B.I., Beachy, P.A., 1994. Autoproteolysis in hedgehog protein biogenesis. Science (New York, N.Y 266, 1528–1537.
Lee, Y., Miller, H.L., Russell, H.R., Boyd, K., Curran, T., McKinnon, P.J., 2006. Patched2 modulates tumorigenesis in patched1 heterozygous mice. Cancer research 66, 6964–6971. doi:10.1158/0008-5472.CAN-06-0505
Lipinski, R.J., Bijlsma, M.F., Gipp, J.J., Podhaizer, D.J., Bushman, W., 2008. Establishment and characterization of immortalized Gli-null mouse embryonic fibroblast cell lines. BMC cell biology 9, 49.
Maun, H.R., Wen, X., Lingel, A., de Sauvage, F.J., Lazarus, R.A., Scales, S.J., Hymowitz, S.G., 2010. Hedgehog pathway antagonist 5E1 binds hedgehog at the pseudo-active site. The Journal of biological chemistry 285, 26570–26580.
McLellan, J.S., Zheng, X., Hauk, G., Ghirlando, R., Beachy, P.A., Leahy, D.J., 2008. The mode of Hedgehog binding to Ihog homologues is not conserved across different phyla. Nature 455, 979–983.
Meyer, N.P., Roelink, H., 2003. The amino-terminal region of Gli3 antagonizes the Shh response and acts in dorsoventral fate specification in the developing spinal cord. Developmental biology 257, 343–355.
Milenkovic, L., Scott, M.P., Rohatgi, R., 2009. Lateral transport of Smoothened from the plasma membrane to the membrane of the cilium. The Journal of cell biology 187, 365–374.
Myers, B.R., Sever, N., Chong, Y.C., Kim, J., Belani, J.D., Rychnovsky, S., Bazan, J.F., Beachy, P.A., 2013. Hedgehog pathway modulation by multiple lipid binding sites on the smoothened effector of signal response. Developmental cell 26, 346–357. doi:10.1016/j.devcel.2013.07.015
Nachtergaele, S., Mydock, L.K., Krishnan, K., Rammohan, J., Schlesinger, P.H., Covey, D.F., Rohatgi, R., 2012. Oxysterols are allosteric activators of the oncoprotein Smoothened. Nature chemical biology 8, 211–220. doi:10.1038/nchembio.765
Nachtergaele, S., Whalen, D.M., Mydock, L.K., Zhao, Z., Malinauskas, T., Krishnan, K., Ingham, P.W., Covey, D.F., Siebold, C., Rohatgi, R., 2013. Structure and function of the Smoothened extracellular domain in vertebrate Hedgehog signaling. Elife 2, e01340.

doi:10.7554/eLife.01340
Nedelcu, D., Liu, J., Xu, Y., Jao, C., Salic, A., 2013. Oxysterol binding to the extracellular domain of Smoothened in Hedgehog signaling. Nature chemical biology. doi:10.1038/nchembio.1290
Odent, S., Atti Bitach, T., Blayau, M., Mathieu, M., Aug, J., Delezo de, A.L., Gall, J.Y., Le Marec, B., Munnich, A., David, V., Vekemans, M., 1999. Expression of the Sonic hedgehog (SHH) gene during early human development and phenotypic expression of new mutations causing holoprosencephaly. Hum. Mol. Genet. 8, 1683–1689.
Ohlig, S., Farshi, P., Pickhinke, U., van den Boom, J., Höing, S., Jakuschev, S., Hoffmann, D., Dreier, R., Schöler, H.R., Dierker, T., Bordych, C., Grobe, K., 2011. Sonic hedgehog shedding results in functional activation of the solubilized protein. Developmental cell 20, 764–774. doi:10.1016/j.devcel.2011.05.010
Ohlig, S., Pickhinke, U., Sirko, S., Bandari, S., Hoffmann, D., Dreier, R., Farshi, P., Götz, M., Grobe, K., 2012. An emerging role of Sonic hedgehog shedding as a modulator of heparan sulfate interactions. The Journal of biological chemistry 287, 43708–43719. doi:10.1074/jbc.M112.356667
Pettigrew, C.A., Asp, E., Emerson, C.P., 2014. A new role for Hedgehogs in juxtacrine signaling. Mechanisms of development 131, 137–149. doi:10.1016/j.mod.2013.12.002
Porter, J.A., Ekker, S.C., Park, W.J., Kessler, von, D.P., Young, K.E., Chen, C.H., Ma, Y., Woods, A.S., Cotter, R.J., Koonin, E.V., Beachy, P.A., 1996. Hedgehog patterning activity: role of a lipophilic modification mediated by the carboxy-terminal autoprocessing domain. Cell 86, 21–34.
Ran, F.A., Hsu, P.D., Wright, J., Agarwala, V., Scott, D.A., Zhang, F., 2013. Genome engineering using the CRISPR-Cas9 system. Nat Protoc 8, 2281–2308. doi:10.1038/nprot.2013.143
Rebollido-Rios, R., Bandari, S., Wilms, C., Jakuschev, S., Vortkamp, A., Grobe, K., Hoffmann, D., 2014. Signaling domain of Sonic Hedgehog as cannibalistic calcium-regulated zinc-peptidase. PLoS Comput. Biol. 10, e1003707. doi:10.1371/journal.pcbi.1003707
Roberts, B., Casillas, C., Alfaro, A.C., Jägers, C., roelink, H., 2016. Patched1 and Patched2 inhibit Smoothened non-cell autonomously. Elife 5, e17634. doi:10.7554/eLife.17634
Roelink, H., Porter, J.A., Chiang, C., Tanabe, Y., Chang, D.T., Beachy, P.A., Jessell, T.M., 1995. Floor plate and motor neuron induction by different concentrations of the amino-terminal cleavage product of sonic hedgehog autoproteolysis. Cell 81, 445–455.
Roessler, E., El-Jaick, K.B., Dubourg, C., Vélez, J.I., Solomon, B.D., Pineda-Alvarez, D.E., Lacbawan, F., Zhou, N., Ouspenskaia, M., Paulussen, A., Smeets, H.J., Hehr, U., Bendavid, C., Bale, S., Odent, S., David, V., Muenke, M., 2009. The mutational spectrum of holoprosencephaly-associated changes within the SHH gene in humans predicts loss-of-function through either key structural alterations of the ligand or its altered synthesis. Hum. Mutat. 30, E921–35. doi:10.1002/humu.21090
Rohatgi, R., Milenkovic, L., Scott, M.P., 2007. Patched1 regulates hedgehog signaling at the primary cilium. Science (New York, N.Y 317, 372–376.
Ruiz i Altaba, A., 1998. Combinatorial Gli gene function in floor plate and neuronal inductions by Sonic hedgehog. Development (Cambridge, England) 125, 2203–2212.
Sasaki, H., Hui, C., Nakafuku, M., Kondoh, H., 1997. A binding site for Gli proteins is essential for HNF-3beta floor plate enhancer activity in transgenics and can respond to Shh in vitro. Development (Cambridge, England) 124, 1313–1322.
Sharpe, H.J., Wang, W., Hannoush, R.N., de Sauvage, F.J., 2015. Regulation of the oncoprotein Smoothened by small molecules. Nature chemical biology 11, 246–255. doi:10.1038/nchembio.1776
Shaw, A., Gipp, J., Bushman, W., 2009. The Sonic Hedgehog pathway stimulates prostate tumor growth by paracrine signaling and recapitulates embryonic gene expression in tumor myofibroblasts. Oncogene 28, 4480–4490.
Singh, S., Tokhunts, R., Baubet, V., Goetz, J.A., Huang, Z.J., Schilling, N.S., Black, K.E., MacKenzie, T.A., Dahmane, N., Robbins, D.J., 2009. Sonic hedgehog mutations identified in

holoprosencephaly patients can act in a dominant negative manner. Hum. Genet. 125, 95–103. doi:10.1007/s00439-008-0599-0
Stamataki, D., Ulloa, F., Tsoni, S.V., Mynett, A., Briscoe, J., 2005. A gradient of Gli activity mediates graded Sonic Hedgehog signaling in the neural tube. Genes & development 19, 626–641. doi:10.1101/gad.325905
Taipale, J., Cooper, M.K., Maiti, T., Beachy, P.A., 2002. Patched acts catalytically to suppress the activity of Smoothened. Nature 418, 892–897.
Traiffort, E., Dubourg, C., Faure, H., Rognan, D., Odent, S., Durou, M.-R., David, V., Ruat, M., 2004. Functional characterization of sonic hedgehog mutations associated with holoprosencephaly. J. Biol. Chem. 279, 42889–42897. doi:10.1074/jbc.M405161200
Tukachinsky, H., Petrov, K., Watanabe, M., Salic, A., 2016. Mechanism of inhibition of the tumor suppressor Patched by Sonic Hedgehog. Proceedings of the National Academy of Sciences of the United States of America 113, E5866–E5875. doi:10.1073/pnas.1606719113
van Heijenoort, J., 2011. Peptidoglycan hydrolases of Escherichia coli. Microbiol. Mol. Biol. Rev. 75, 636–663. doi:10.1128/MMBR.00022-11
Wichterle, H., Lieberam, I., Porter, J.A., Jessell, T.M., 2002. Directed differentiation of embryonic stem cells into motor neurons. Cell 110, 385–397.
Xiao, X., Tang, J.-J., Peng, C., Wang, Y., Fu, L., Qiu, Z.-P., Xiong, Y., Yang, L.-F., Cui, H.-W., He, X.-L., Yin, L., Qi, W., Wong, C.C.L., Zhao, Y., Li, B.-L., Qiu, W.-W., Song, B.-L., 2017. Cholesterol Modification of Smoothened Is Required for Hedgehog Signaling. Molecular cell 66, 154–162.e10. doi:10.1016/j.molcel.2017.02.015
Yauch, R.L., Gould, S.E., Scales, S.J., Tang, T., Tian, H., Ahn, C.P., Marshall, D., Fu, L., Januario, T., Kallop, D., Nannini-Pepe, M., Kotkow, K., Marsters, J.C., Rubin, L.L., de Sauvage, F.J., 2008. A paracrine requirement for hedgehog signalling in cancer. Nature 455, 406–410.
Zhang, J., Rosenthal, A., de Sauvage, F.J., Shivdasani, R.A., 2001. Downregulation of Hedgehog signaling is required for organogenesis of the small intestine in Xenopus. Developmental biology 229, 188–202.
Zhang, X.M., Ramalho-Santos, M., McMahon, A.P., 2001. Smoothened mutants reveal redundant roles for Shh and Ihh signaling including regulation of L/R asymmetry by the mouse node. Cell 105, 781–792.

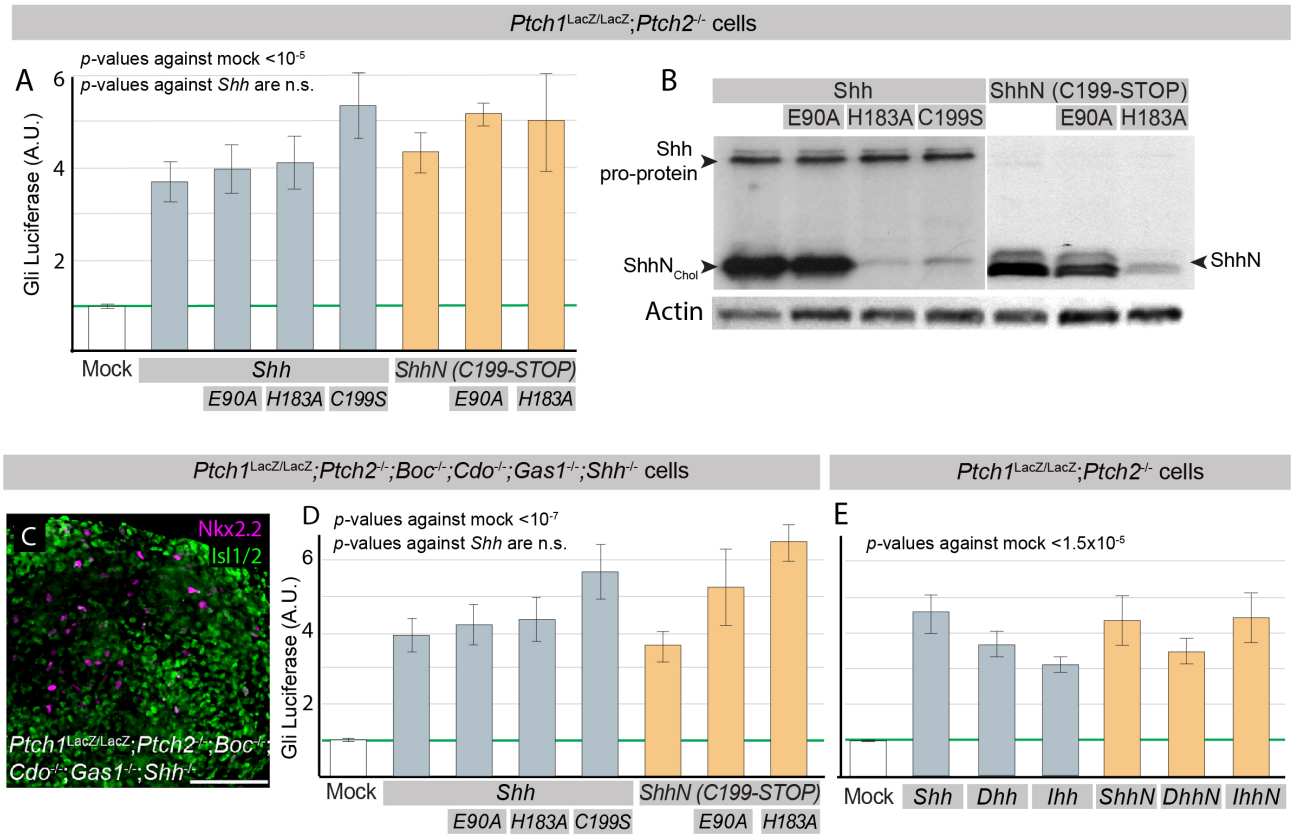

Figure 1. Shh mutants affecting the cholesterol moiety or the metal coordination sites gain the ability to activate the Hh response in cells lacking Hh receptors

(A) *Ptch1*$^{LacZ/LacZ}$;*Ptch2*$^{-/-}$ cells were transfected with *Gli-Luciferase* (*Luc*) alone (Mock) or co-transfected with *Gli-Luc* and *Shh*, *Shh-E90A*, *Shh-H183A, ShhN, ShhN-E90A, or ShhN-H183A*. Luciferase levels in mock transfected *Ptch1*$^{LacZ/LacZ}$;*Ptch2*$^{-/-}$ cells were set at "1". (B) Western blot analysis of Shh, Shh-E90A, Shh-H183A, Shh-C199A, ShhN, ShhN-E90A, and ShhN-H183A protein expression in *Ptch1*$^{LacZ/LacZ}$;*Ptch2*$^{-/-}$ cells, using an antibody directed against the N-terminal domain of Shh. (C) Neuralized Embryoid body derived from *Ptch1*$^{LacZ/LacZ}$;*Ptch2*$^{-/-}$;*Boc*$^{-/-}$;*Cdo*$^{-/-}$;*Gas1*$^{-/-}$;*Shh*$^{-/-}$ mESCs. Expression of Nkx2.2 and Olig2 was assessed by immunofluorescence after 5 days in culture. (D) *Ptch1*$^{LacZ/LacZ}$;*Ptch2*$^{-/-}$;*Boc*$^{-/-}$;*Cdo*$^{-/-}$;*Gas1*$^{-/-}$;*Shh*$^{-/-}$ cells were transfected with *Gli-Luc* alone (Mock) or co-transfected with *Gli-Luc* and *Shh*, *Shh-E90A*, *Shh-H183A*, *ShhN*, *ShhN-E90A*, or *ShhN-H183A*. Luciferase levels in Mock transfected cells were set at "1". (I) *Ptch1*$^{LacZ/LacZ}$;*Ptch2*$^{-/-}$ cells were transfected with *Gli-Luc* alone (Mock) or co-transfected with *Gli-Luc* and *ShhN*, *DhhN*, *IhhN*, *Shh*, *Dhh*, *or Ihh.* Luciferase levels in Mock transfected cells were set at "1". All error bars are s.e.m., *p* values (Student t-test, 2 tailed) against mock are indicated were relevant, (A) n≥25, (D) n≥11, (E) n≥6, all independent biological replicates.

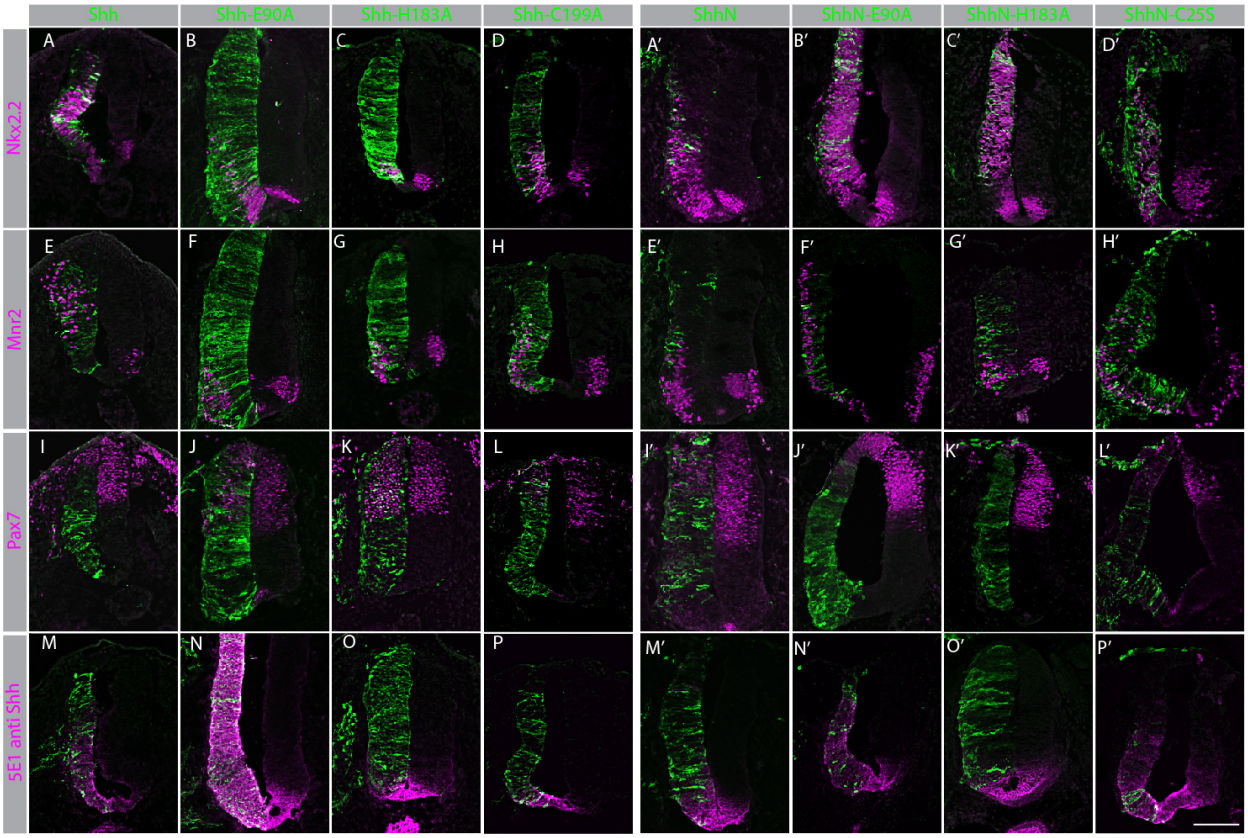

Figure 2. Shh and ShhN mutants activate the Hh pathway *in vivo* independent of receptor binding

(Panels A-P) Cross-sections of stage 20 HH chicken neural tubes co-electroporated with *GFP* and *Shh* (A, E, I, M), *Shh-E90A* (B, F, J, N), *Shh-H183A* (C, G, K, O), or *Shh-C199A* (*C199A* (D, H, L, P), labeled in green). Sections are stained with antibodies to Nkx2.2 (A-D), Mnr2 (E-H), Pax7 (I-L), and Shh (5E1) (M-P) labeled in magenta. (Panels A'-P') Cross-sections of stage 20 HH chicken neural tubes co-electroporated at stage 10 with *GFP* and *ShhN* (A',E',I',M'), *ShhN-E90A* (B',F',J',N'), or *ShhN-H183A* (C',G',K',O'). *ShhN-C25S* (D',H',L',P') labeled in green. Sections are stained with antibodies to Nkx2.2 (A-D, A'-D'), Mnr2 (E-H, E'-H'), Pax7 (I-L, I'-L'), and Shh (5E1) (M-P, M'-P') labeled in magenta. Scale bar is 100μm.

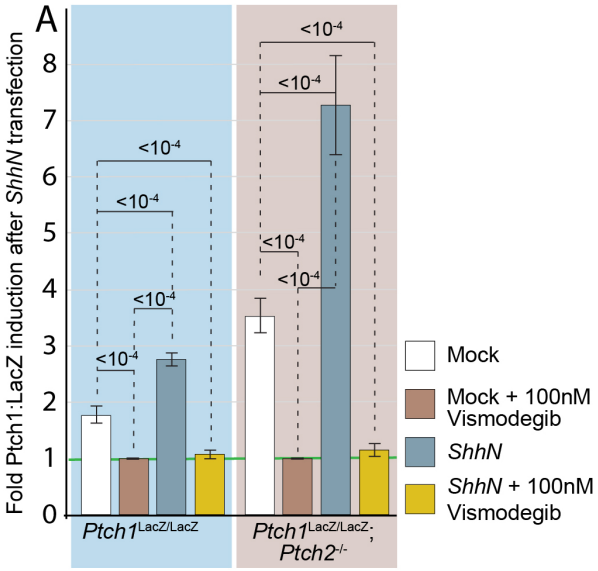
A
Fold Ptch1:LacZ induction after ShhN transfection
0
1
2
3
4
5
6
7
8
<10-4
Mock
Mock + 100nM Vismodegib
ShhN
ShhN + 100nM Vismodegib
Ptch1LacZ/LacZ
Ptch1LacZ/LacZ; Ptch2-/-

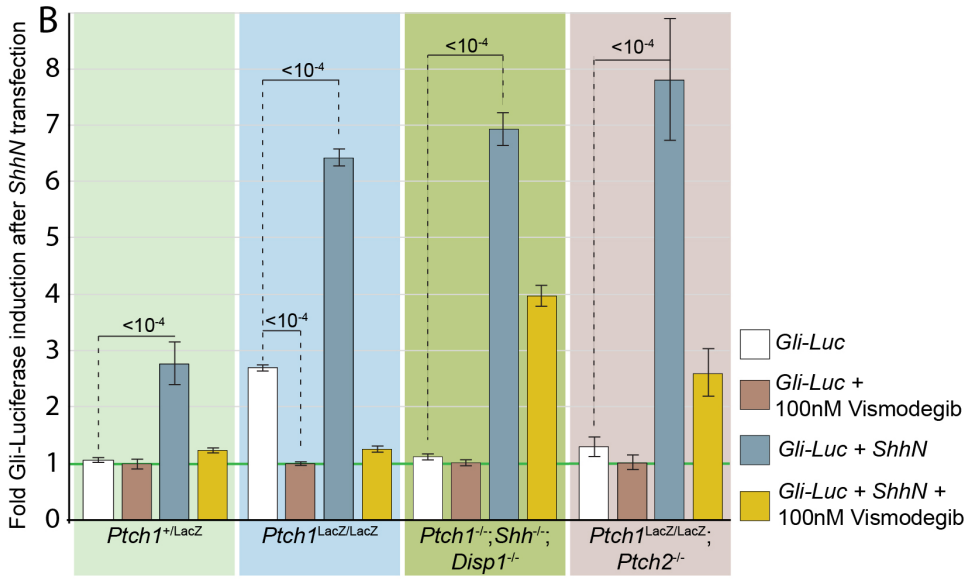
B
Fold Gli-Luciferase induction after ShhN transfection
0
1
2
3
4
5
6
7
8
<10-4
Gli-Luc
Gli-Luc + 100nM Vismodegib
Gli-Luc + ShhN
Gli-Luc + ShhN + 100nM Vismodegib
Ptch1+/LacZ
Ptch1LacZ/LacZ
Ptch1-/-; Shh-/-; Disp1-/-
Ptch1LacZ/LacZ; Ptch2-/-

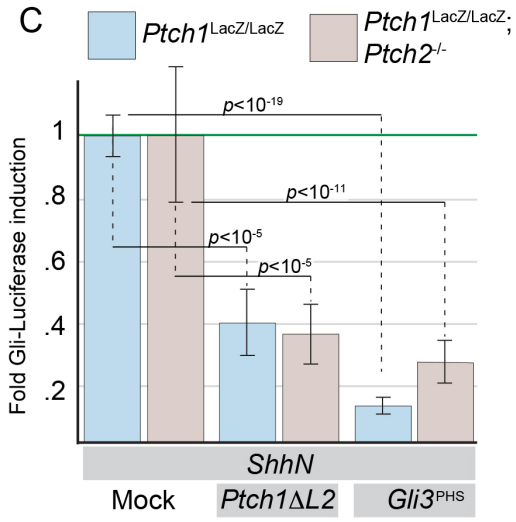
C
Ptch1LacZ/LacZ
Ptch1LacZ/LacZ; Ptch2-/-
Fold Gli-Luciferase induction
.2
.4
.6
.8
1
p<10-19
p<10-11
p<10-5
p<10-5
ShhN
Mock
Ptch1ΔL2
Gli3PHS

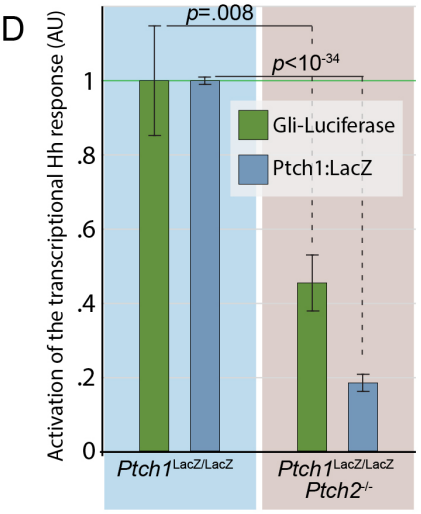
D
Activation of the transcriptional Hh response (AU)
0
.2
.4
.6
.8
1
p=.008
p<10-34
Gli-Luciferase
Ptch1:LacZ
Ptch1LacZ/LacZ
Ptch1LacZ/LacZ Ptch2-/-

Figure 3. Activation of the Hh response by ShhN does not require Ptch1/2 activity

(A) *Ptch1*$^{LacZ/LacZ}$ cells and *Ptch1*$^{LacZ/LacZ}$;*Ptch2*$^{-/-}$ (indicated) were assessed for Ptch1:LacZ expression after mock transfection (white and brown bars) or *ShhN* transfection (blue and yellow bars). Each condition was treated with either a Smo inhibitor, 100 nM Vismodegib (brown and yellow bars), or a DMSO vehicle control (white and blue bars). β-Gal levels in mock transfected cells treated with 100 nM Vismodegib for each cell line were set at "1". (B) *Ptch1*$^{+/LacZ}$ cells, *Ptch1*$^{LacZ/LacZ}$ cells, *Ptch1*$^{-/-}$;*Shh*$^{-/-}$;*Disp1*$^{-/-}$, and *Ptch1*$^{LacZ/LacZ}$;*Ptch2*$^{-/-}$ cells (indicated) were co-transfected with *Gli-Luc* and *GFP* (Mock; white/brown bars) or co-transfected with *Gli-Luc* and *ShhN* (blue and yellow bars). Each condition was treated with either a Smo inhibitor, 100 nM Vismodegib (brown and yellow bars), or a DMSO vehicle control (white and blue bars). Luciferase levels in mock transfected cells treated with 100 nM Vismodegib for each cell line were set at "1". (C) Gli-luc levels were assayed in *Ptch1*$^{LacZ/LacZ}$ (blue bars) and *Ptch1*$^{LacZ/LacZ}$;*Ptch2*$^{-/-}$ (pink bars) transfected with *Ptch1ΔL2*,*or Gli3*^{phs} together with *Gli-luc* and *ShhN*. Luciferase levels in *ShhN*, mock co-transfected cells were set at "1" for each cell line. (D) Hh pathway activation in *Ptch1*$^{LacZ/LacZ}$ and *Ptch1*$^{LacZ/LacZ}$;*Ptch2*$^{-/-}$ was measured in parallel using *Gli-luc* and *Ptch1:LacZ.* Using both methods we find higher Hh pathway activation in the *Ptch1*$^{LacZ/LacZ}$ cells than the *Ptch1*$^{LacZ/LacZ}$;*Ptch2*$^{-/-}$ cells. Luciferase and LacZ levels in *Ptch1*$^{LacZ/LacZ}$ cells were set at "1". Error bars are s.e.m., *p*-values (Student t-test, 2 tailed) are indicated were relevant, n=6 for Gli-Luc assay, n≥25 for LacZ assay, all independent biological replicates. All error bars are s.e.m., *p*-values (Student t-test, 2 tailed) are indicated where relevant, (A) n≥4, (B) n≥9, (C) n≥13, n≥8 all independent biological replicates.

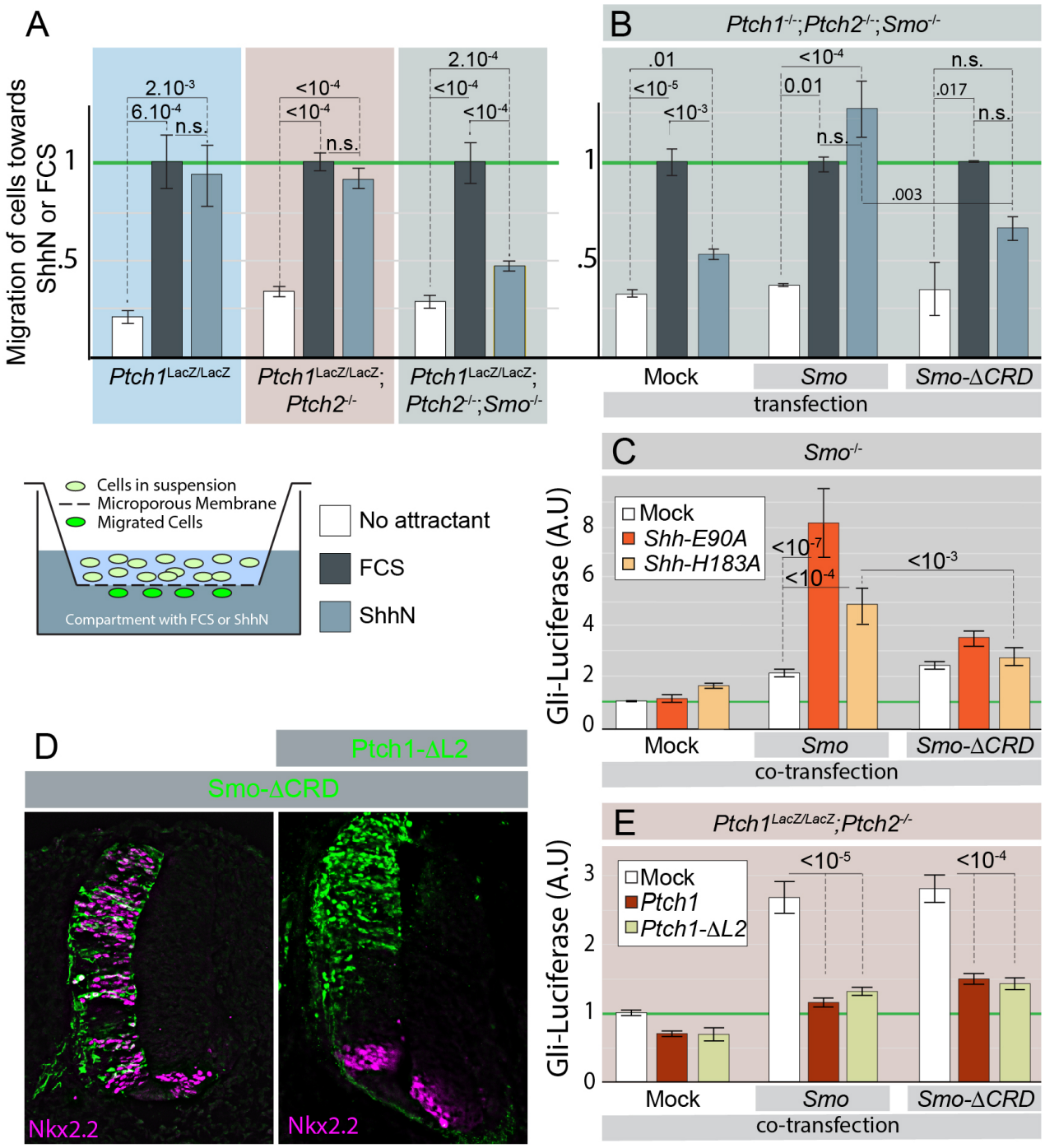
A
Migration of cells towards ShhN or FCS
1
.5
2.10-3
6.10-4
n.s.
<10-4
<10-4
n.s.
2.10-4
<10-4
<10-4
Ptch1LacZ/LacZ
Ptch1LacZ/LacZ; Ptch2-/-
Ptch1LacZ/LacZ; Ptch2-/-;Smo-/-
B
Ptch1-/-;Ptch2-/-;Smo-/-
.01
<10-5
<10-3
<10-4
0.01
n.s.
.003
n.s.
.017
n.s.
Mock
Smo
Smo-ΔCRD
transfection
Cells in suspension
Microporous Membrane
Migrated Cells
Compartment with FCS or ShhN
No attractant
FCS
ShhN
C
Smo-/-
Gli-Luciferase (A.U)
0
2
4
6
8
Mock
Shh-E90A
Shh-H183A
<10-7
<10-4
<10-3
Mock
Smo
Smo-ΔCRD
co-transfection
D
Ptch1-ΔL2
Smo-ΔCRD
Nkx2.2
Nkx2.2
E
Ptch1LacZ/LacZ;Ptch2-/-
Gli-Luciferase (A.U)
0
1
2
3
Mock
Ptch1
Ptch1-ΔL2
<10-5
<10-4
Mock
Smo
Smo-ΔCRD
co-transfection

Figure 4. Smo∆CRD retains sensitivity to Ptch1-mediated inhibition in vitro and in vivo, but cannot be activated by Shh in aPtch1/2-independent manner

(A) Cells with the indicated genotypes were assayed in a modified Boyden chamber (diagram) for their ability to migrate towards FCS or ShhN. Migration was normalized to FCS for each condition. (B) *Ptch1*$^{-/-}$;*Ptch2*$^{-/-}$;*Smo*$^{-/-}$ cells were mock transfected, or transfected with *Smo* or *Smo-∆CRD*. The transfected cells were assayed in a modified Boyden chamber for their ability to migrate towards FCS or ShhN. (C) *Smo*$^{-/-}$ cells were transfected with *Gli-Luc,* and co-transfected with *Smo* or *Smo-∆CRD and Shh-E90A* or *Shh-H183A* as indicated. Gli-Luciferase levels were quantified, and the levels in double mock transfected cells set at "1". (D) Stage 10 chicken embryos were electroporated with *Smo-∆CRD* (green) or co-electroporated with *Smo-∆CRD* and *Ptch1-∆L2 (Green)*. The ventral marker NKX2.2 was visualized (purple). (E) *Ptch1*$^{LacZ/LacZ}$;*Ptch2*$^{-/-}$ cells were transfected with *Gli-Luc,* and co-transfected with *Smo* or *Smo-∆CRD, and Ptch1* or *Ptch1-∆L2* as indicated. Gli-Luciferase levels were quantified, and the levels in mock/mock/*Gli-Luc* transfected cells set at "1".

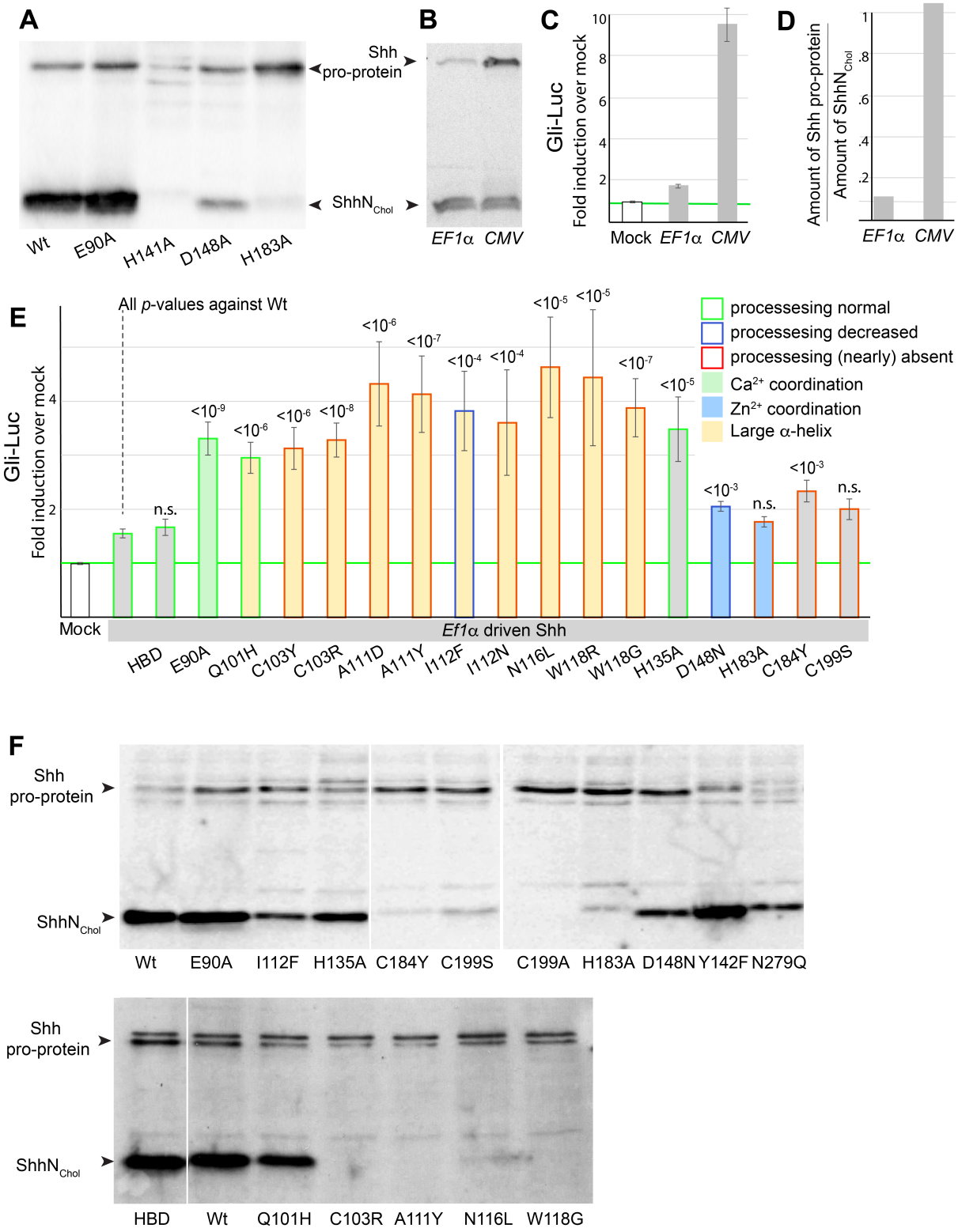
A
Shh
pro-protein
ShhN$_{Chol}$
Wt
E90A
H141A
D148A
H183A
B
EF1α
CMV
C
Gli-Luc
Fold induction over mock
Mock
EF1α
CMV
D
Amount of Shh pro-protein
Amount of ShhN$_{Chol}$
EF1α
CMV
E
All p-values against Wt
Gli-Luc
Fold induction over mock
processesing normal
processesing decreased
processesing (nearly) absent
Ca^{2+} coordination
Zn^{2+} coordination
Large α-helix
Mock
Ef1α driven Shh
HBD
E90A
Q101H
C103Y
C103R
A111D
A111Y
I112F
I112N
N116L
W118R
W118G
H135A
D148N
H183A
C184Y
C199S
F
Shh
pro-protein
ShhN$_{Chol}$
Wt
E90A
I112F
H135A
C184Y
C199S
C199A
H183A
D148N
Y142F
N279Q
Shh
pro-protein
ShhN$_{Chol}$
HBD
Wt
Q101H
C103R
A111Y
N116L
W118G

Figure 5. Shh processing is not required for the cell-autonomous activation of the Hh response. (A) Mutations in the Zn^{2+} coordination triad (H141A, D148A, H183A) severely compromise, or prevent Shh processing. E90A (affecting Ca^{2+} coordination) undergoes normal processing. (B) Shh expression levels (high for the *CMV* and low for the *EF1*α promoter) affect the level of Shh pro-protein more so than $ShhN_{Chol}$. (C) The induction of the cell autonomous Hh response correlates with the amount of observed Shh pro-protein, but not Shh_{Chol}. (D) Ratio of Shh pro-protein over $ShhN_{Chol}$. (E) All Shh mutants are driven off the *EF1*α promoter. Activity to induce the Hh response *in cis* of several holoprosencephaly mutants located in the large α-helix (C103Y, C103R A111D, A111Y, I112F, I112N, N116L, W118R, W118G), mutants involved in Zn^{2+} coordination (D148N, H183A), E90A (Ca^{2+} coordination), H135 (near the catalytic domain), C184A (commonly mutated in holoprosencephaly), and C199S (cleavage site for auto-processing), Shh HBD (K38S, K39S, K179S) was used as a control. (F) Western blot analysis of *EF1*α-driven Shh mutants assessed in F. Note that the ability to auto-process is often impaired in α-helix and Zn^{2+} coordination mutants.

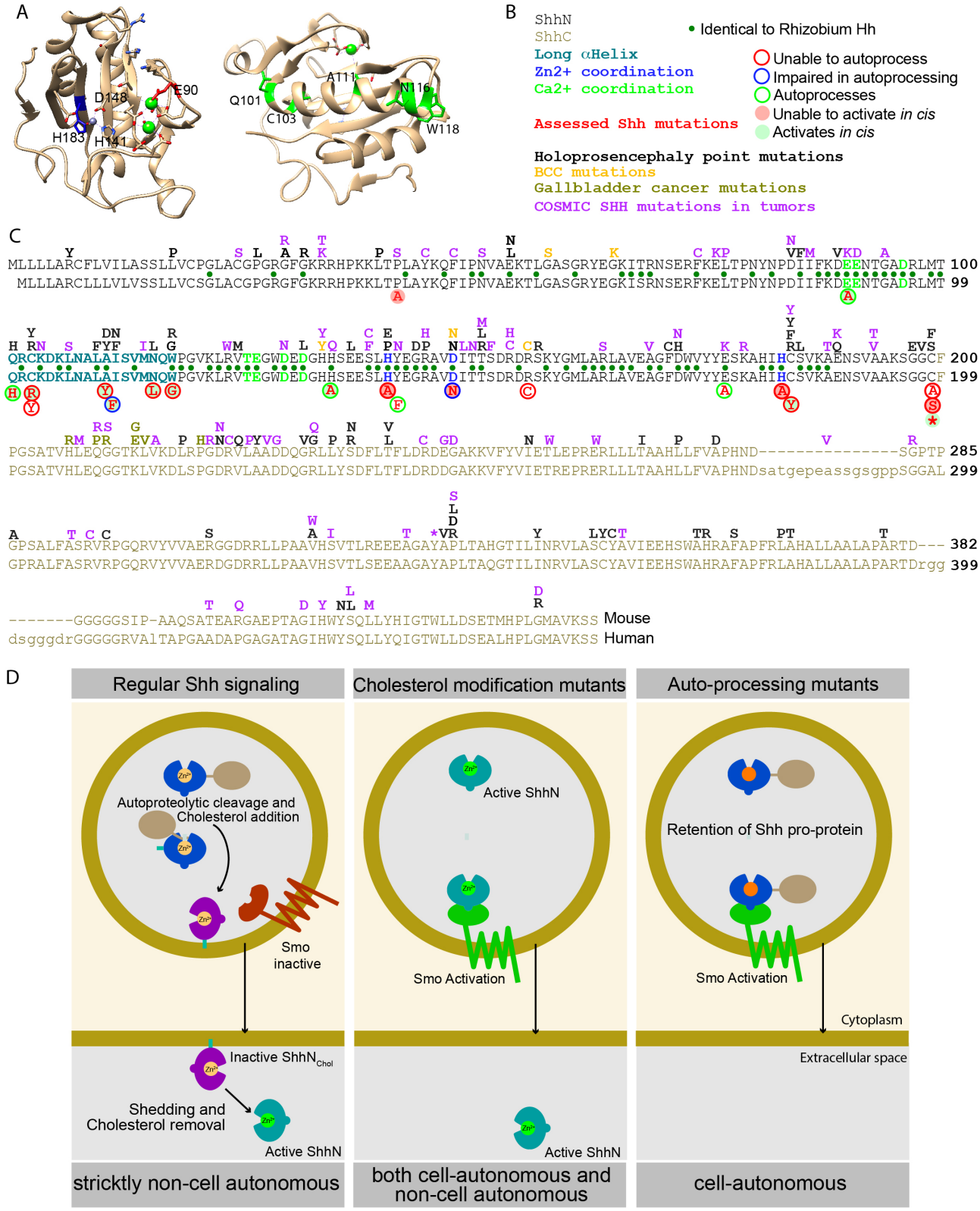
A
D148
E90
H183
H141
Q101
C103
A111
N116
W118
B
ShhN
ShhC
Long αHelix
Zn2+ coordination
Ca2+ coordination
Assessed Shh mutations
Identical to Rhizobium Hh
Unable to autoprocess
Impaired in autoprocessing
Autoprocesses
Unable to activate in cis
Activates in cis
Holoprosencephaly point mutations
BCC mutations
Gallbladder cancer mutations
COSMIC SHH mutations in tumors
C
Mouse
Human
D
Regular Shh signaling
Cholesterol modification mutants
Auto-processing mutants
Autoproteolytic cleavage and Cholesterol addition
Smo inactive
Inactive ShhN Chol
Shedding and Cholesterol removal
Active ShhN
Active ShhN
Smo Activation
Active ShhN
Retention of Shh pro-protein
Smo Activation
Cytoplasm
Extracellular space
stricktly non-cell autonomous
both cell-autonomous and non-cell autonomous
cell-autonomous

Figure 6. Overview and model. Representation of the ShhN crystal structure with salient residues indicated. On the left is a view into the Zn^{2+} (grey)/Ca^{2+} (green) coordination domains, on the right is the opposite view with the large α-helix in front, with mutated residues indicated in green. (B, C) Lineup of the mouse (top) and human Shh. All tested mutants are indicated below the lineup, with their activity and ability to process indicated. Above the line are Shh point mutations described for holoprosencephaly, BCCs, Gallbladder Cancers, and those curated in the COSMIC database. Identical residues found in *Mesorhizobium* Hh are indicated with green dots between the lines. (D) During regular Hh signaling, the potentially active pro-protein autocleaves to yield the inactive Shh_{Chol} form. Further processing mediates activation and release, thus allowing signaling *in trans*. Mutants that do not receive the cholesterol modification always exist in an active form, thus mediating both *c*ell-autonomous and non-cell autonomous signaling. Repressed autoprocessing of the Shh pro-protein results in perdurance of this active form, thus causing cell-autonomous activation of the Hh response.